

# 國立交通大學

電信工程學系

碩士論文

基於幾何特性輔助的無線定位演算法



Geometry-Assisted Location Estimation Algorithms  
in Wireless Networks

研究生：朱林志

指導教授：方凱田 教授

中華民國九十七年六月

基於幾何特性輔助的無線定位演算法

Geometry-Assisted Location Estimation Algorithms in Wireless  
Networks

研 究 生：朱林志

Student : Lin-Chin Chu

指導教授：方凱田

Advisor : Kai-Ten Feng

國 立 交 通 大 學

電信工程學系碩士班

碩 士 論 文



Submitted to Department of Computer and Information Science

College of Electrical Engineering and Computer Science

National Chiao Tung University

in partial Fulfillment of the Requirements

for the Degree of

Master

in

Communication Engineering

June 2008

Hsinchu, Taiwan, Republic of China

中華民國九十七年六月

# 基於幾何特性輔助的無線定位演算法

學生：朱林志

指導教授：方凱田

國立交通大學電信工程學系（研究所）碩士班

## 摘 要

近幾年來，無線定位估測吸引了許多領域的研究目光，而以網路架構為基礎，利用發送訊號來作為移動者和基地台間彼此的溝通方式，這種定位方式更被廣泛的應用。在以往的研究方式，二階最小平方定位法 (two-step Least Square Estimation) 廣為大家所應用的一種，並提供了移動者有效的定位計算。但是此種演算法在不好的幾何環境下會使精準度產生偏差，利用兩種幾何的指標：幾何衰減效應 (GDOP) 和幾何量測優勢分析 (GDOP MOM)，作為本篇論文的分析標準。在文章中，我們建立了幾何輔助演算法 (GALE)，藉由基地台和移動者間的幾何相關位置，來達到使 GDOP 和 MOM 這兩個幾何指標最小值的方式，藉由 two-step LS 重新找出虛構的基地台群集。幾何輔助演算法 (GALE) 演算法尤其用在較差的幾何特性時能大大的提升了 two-step LS 的定位精準度，並且節省了量測時間，在最後一章節的模擬分析中，可以發現 GALE 在網路定位環境中的優越點。


# Geometry-Assisted Location Estimation Algorithms in Wireless Networks

Student : Lin-Chih Chu

Advisor : Dr. Kai-Ten Feng

Department ( Institute ) of Communication Engineering  
National Chiao Tung University

## ABSTRACT



In recent years, wireless location estimation has attracted a significant amount of attention in different areas. The network-based location estimation schemes have been widely adopted based on the radio signals between the mobile station (MS) and the base stations (BSs). The two-step Least Square (LS) method has been studied in related research to provide efficient location estimation of the MS. However, the algorithm results in inaccurate location estimation under the circumstances with poor geometry property such as two indexes, the geometric dilution of precision (GDOP) and the GDOP measure-of-merit (MOM). In this paper, the geometry-assisted location estimation (GALE) schemes are proposed by considering the geometric relationships between the MS and its associated BSs. According to the minimal GDOP and MOM criterion, the BSs are fictitiously repositioned and are served as a new set of BSs within the formulation of the two-step LS algorithm. The proposed GALE schemes can both preserve the computational efficiency from the two-step LS method and obtain precise location estimation under poor geometric environments. Comparing with other existing schemes, numerical results demonstrate that the proposed GALE algorithms can achieve better accuracy in wireless location estimation.

# 致 謝

碩士班的兩年就這樣過去了，兩年前懵懂無知，只會追尋課本知識的我就這樣進入了交大這個學術界的偉大殿堂，感謝我的指導教授方凱田老師，將我督促到了今天畢業，平時許多的建議，都是今天能完成這一本論文的最大助力。也謝謝我的口試委員：電子系的黃經堯老師和資工系的趙禧緣老師，點出了許多這篇論文還未完整的部分，都是幫助我未來讓研究能更完整的方向。

實驗室的學長，伯軒、建華、昭霖三位學長在 meeting 時幫助我找出研究方向、並能不時的給予知識上的提供，讓我在找尋資料上節省了許多的時間，文俊、裕彬、仲賢學長在平時不斷的鼓勵、研究上的建議，在這兩年的碩士生涯間，都是我研究的動力。學弟們，瑞廷、佳仕、俊傑、佳偉平時在實驗室帶給我們的歡樂，還有隔壁實驗室冠勳、紘睿、綱綸、冠螢以及許多的朋友們，曾經在研究苦悶的時候，陪我出去走走，一起打球抒發壓力，有了這種種的一切，構成了我這兩年的研究所生活。

更要感謝的是我的父母，容忍著這久久才回家一次的小孩，你們的諒解讓我能安心的完成我的學業。

學習的路上，有了你們，真好。

朱林志謹誌

于交通大學  
2008.06

# Contents

中文提要 .....	i
英文提要 .....	ii
誌謝 .....	iii
目錄 .....	iv
圖目錄 .....	vi
<b>1 Introduction</b> .....	<b>1</b>
<b>2 Related work</b> .....	<b>6</b>
2.1 Studies on Propagation Noise .....	6
2.2 Studies on Existing Location Estimation Algorithms .....	8
2.2.1 Taylor-Series Estimation .....	9
2.2.2 Two-Step Least Square Method .....	11
2.2.3 Geometry-Constrained Location Estimation (GLE) Algorithm .....	15
<b>3 Derivation from GDOP and GDOP MOM Metric</b> .....	<b>20</b>
3.1 Mathematical Modeling .....	20
3.2 Geometric Dilution of Precision (GDOP) .....	24
3.2.1 Derived GDOP property .....	25
3.3 GDOP Measure-of-Merit (MOM) .....	30
3.3.1 Derived MOM property .....	32
<b>4 Proposed Geometric-Assisted Location Estimation (GALE)</b> <b>Algorithms</b> .....	<b>37</b>

4.1 GALE with One Movable Fictitious BS Scheme . . . . .	38
4.1.1 GDOP-Assisted (GOLE) Location Estimation Scheme . . . . .	40
4.1.2 MOM-Assisted (MOLE) Location Estimation Scheme . . . . .	42
4.1.3 Coverage-Maximize (CMLE) Location Estimation Scheme . . . . .	43
4.2 GALE with Two Movable Fictitious BSs Scheme . . . . .	43
4.2.1 GDOP-Assisted (GOLE) Location Estimation Scheme . . . . .	44
4.2.2 MOM-Assisted (MOLE) Location Estimation Scheme . . . . .	44
4.2.3 Coverage-Maximize (CMLE) Location Estimation Scheme . . . . .	45
5 Performance Evaluation . . . . .	47
5.1 Noise Models . . . . .	47
5.2 Simulation Results . . . . .	48
6 Conclusion . . . . .	53



# List of Figures

1.1 Position determination methods: (a) time of arrival (TOA) (b)time differ-ence of arrival (TDOA) (c) angle of arrival (AOA) . . . . .	6
2.1 The range measurements Su@er from the NLOS errors. . . . .	11
2.2 Geometry of the NLOS error . . . . .	11
2.3 Geometric constraints for TOA-Based location estimation confine the true MS's position in the overlap region of the range measurements. . . . .	20
3.1 Schematic diagram of the network layout for computation. . . . .	26
3.2 GDOP value in a regular pentagon . . . . .	30
3.3 GDOP value in a regular triangle . . . . .	31
3.4 MOM value in a regular pentagon . . . . .	34
3.5 MOM value in a regular triangle . . . . .	35
4.1 Schematic diagram of the proposed GALE algorithms. . . . .	42
4.2 The location information for TOA signal . . . . .	46
5.1 Network topologies for performance evaluation . . . . .	52
5.2 Performance comparison under the LOS environment with both better and worse geometric layouts. . . . .	53
5.3 Performance comparison under the LOS environment with worse geometric layout: Estimation error v.s. standard deviation of measurement noise . . . . .	54
5.4 Performance comparison under the NLOS environment with both better and worse geometric layouts. . . . .	55
5.5 Performance comparison under the NLOS environment with worse geometric layout: Estimation error v.s. median value of NLOS noise. . . . .	55



# Chapter 1

## Introduction

Wireless location technologies [1], which are designated to estimate the position of a mobile station (MS), have drawn a lot of attention over the past few decades. Different types of location-based services (LBSs) [2] have been proposed and studied, including the emergency 911 (E-911) subscriber safety services, the navigation system, and applications for the wireless sensor networks (WSNs) [3]. Due to the emergent interests in the LBSs, it is required to provide enhanced precision in the location estimation of a MS under different environments.

The wireless location techniques can be classified into *(i)* the satellite-based and *(ii)* the network-based location estimation schemes. To simplify the introduction of these techniques, in the following we use two-dimensional (2-D) cases as application examples. A variety of wireless location techniques have been studied and investigated in [1] and the introduction of the wireless location techniques as follows is referred to the research.

The well-adapted technology for the satellite-based location estimation method is to utilize the global positioning systems (GPSs). It measures the time-of-arrival (TOA) of the signals coming from different satellites. The TOA scheme determines the mobile device position based on the intersection of the range circles, as shown in Fig. 1.1a. Since the propagation time of the radio wave is directly proportional to its traversed range,

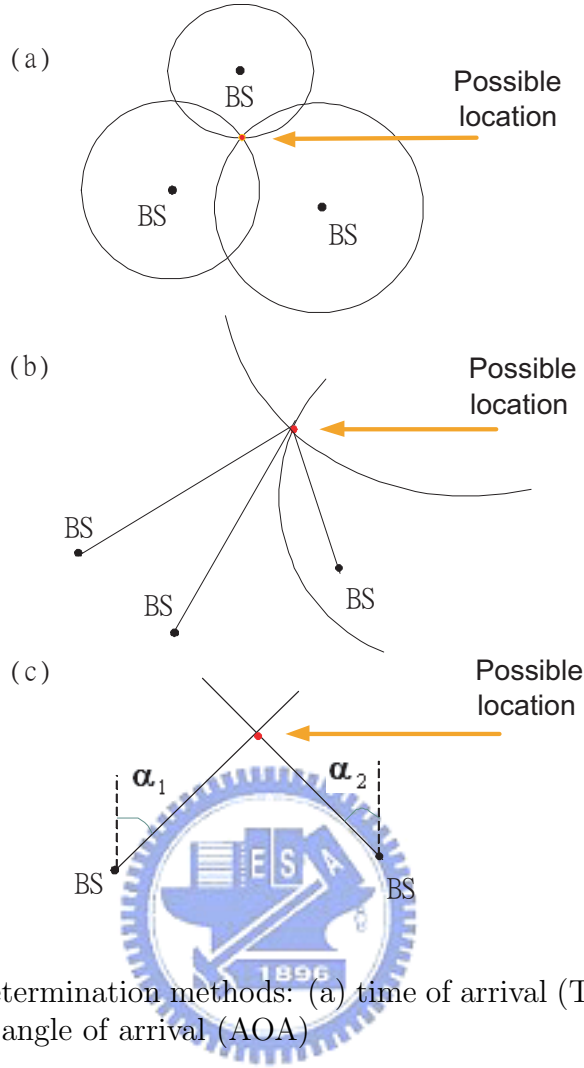


Figure 1.1: Position determination methods: (a) time of arrival (TOA) (b)time difference of arrival (TDOA) (c) angle of arrival (AOA)

multiplying the speed of light to the time can obtain the range from the mobile device to the communicating base station (BS). It is noted that two range measurements provide an ambiguous fix, while three measurements determine a unique position. The same principle is used by GPS, where the circles become the spheres in space and the fourth measurement is required to obtain the 3-D position for mobile device.

The network-based location estimation schemes have been widely proposed and employed in the wireless communication system. These schemes locate the position of the MS based on the measured radio signals from its neighborhood BSs. The representative algorithms for the network-based location techniques are the time difference-of-arrival

(TDOA) and the angle-of-arrival (AOA). The TDOA scheme determines the mobile device position based on the trilateration, as shown in Fig. 1.1b. The scheme uses time difference measurements rather than absolute time measurements as TOA does. It is often referred to as the *hyperbolic system* because the time difference is converted to a constant distance difference to two base stations (as foci) to define a hyperbolic curve. The intersection of two hyperbolas determines the mobile device position. Therefore, it utilizes two pairs of BSs for positioning. The accuracy of the scheme is a function of the relative base station geometric locations. For the network-based systems, it also requires either precisely synchronized clocks for all transmitters and receivers or a means to measure these time differences.

The AOA technique determines the mobile device position based on triangulation, as shown in Fig. 1.1c. It is also called direction of arrival in some literature. The intersection of two directional lines of bearing defines a unique position, each formed by a radial from a BS to the mobile device in the 2-D space. This technique requires a minimum of two BSs to determine a position. If available, more than one pair can be used in practice. However, since directional antennas or antenna arrays are required, it is generally difficult to realize the AOA technique at the mobile device.

A variety of wireless location techniques have been studied and investigated. The network-based location estimation schemes have been widely proposed and employed in the wireless communication system. These algorithms locate the position of the MS based on the measured radio signals either from its neighborhood base stations (BSs) in the cellular-based networks or the sensor nodes (SNs) in the WSNs.

The equations associated with the network-based location estimation schemes are inherently nonlinear. The uncertainties induced by the measurement noises make it more difficult to acquire the MS's estimated position with tolerable precision. Different approaches have been proposed to obtain an approximate location estimation in the previous

studies [4] - [7]. The Taylor series expansion (TSE) method was utilized in [4] to acquire the location estimation from the time measurements. The scheme requires iterative processes to obtain the location estimate from a linearized system. The major drawback of the TSE method is that it may suffer from the convergence problem due to an incorrect initial guess of the MS's position.

The straight line of position (LOP) [7] method presents a different interpretation of the TOA geometry to estimate the MS's location comparing with the conventional circular TOA methods.

The two-step least square (LS) method [5] [6] was adopted as an approximate realization of the maximum likelihood estimator, which does not require iterative processes. It is observed that feasible location estimation can be achieved by adopting these algorithms while the time measurements are symmetrically located w.r.t. the MS. However, asymmetrical measurement inputs to the MS in general result in degraded precision for location estimation. It is especially noticed that this type of situation can frequently occur under non-regular shapes of geometric layouts, e.g. under the randomly distributed sensor networks.

In order to consider the geometric effect to the accuracy of location estimation, the well-known geometric dilution of precision (GDOP) [8] and GDOP MOM [9] metrics can be adopted to facilitate the design of location estimation algorithms. Two metrics are utilized as an index for observing the location precision of the MS under different geometric positions within the networks, e.g. the cellular, the satellite, or the sensor networks. The work in [10] describes the effect and cost resulting from the network topology with significant GDOP values. However, the method for mitigating the GDOP effect has not been extensively addressed in previous studies. The ridge regression signal processing [11] is proposed for reducing the effects of GDOP in the position-fixed navigation systems. Nevertheless, a pre-filtered set of initial range measurements is required before the pro-

posed estimation method can be activated. A new geometric property, coverage, is also introduced in this paper. For the purpose that mitigating estimation error, we use the geometric information to decide the best BS layout and can improve the location system.

In this paper, three Geometric-assisted location estimation (GALE) algorithms are proposed to enhance the estimation precision by incorporating the geometric information within the conventional two-step LS algorithm. Based on an initial estimate of the MS's location, the proposed GALE schemes determine the fictitious locations of the BSs such that the estimated MS will be relocated at a position with the best geometric property, it can be decided by GDOP, MOM or coverage information. According to the these geometric criterion, the GALE(1BS) and GALE(2BS) algorithms are proposed to consider the cases by fictitiously rotating (i.e. not physically relocate) one and two BS's locations respectively. Reasonable location estimation can be acquired within the GALE algorithms, especially feasible for the cases with poor geometric circumstances. Simulation results illustrate that the proposed GALE schemes can achieve higher accuracy for the MS's estimated location compared to the other existing methods.

The remainder of this paper is organized as follows. chapter 3 describes the properties that are derived from the GDOP and GDOP MOM metrics. The proposed GALE algorithms are explained in chapter 4; while chapter 5 shows the performance evaluation of the proposed schemes. chapter 6 draws the conclusions.

# Chapter 2

## Related work

### 2.1 Studies on Propagation Noise

The precision of time measurement significantly leads the performance of the location algorithms which utilize the time-base information. The transmitted radio signal can reach the receiver in the shortest time in the case that there are no barriers in the direct connection between the transmitter and the receiver. This is called the Line-of-Sight (LOS) situation, which often occurs in a open space. Yet, this ideal situation usually can not meet in a obstacle-concentrated environment such as a dense urban or an office inside a building. The emitted radio signal is either reflected or diffracted by obstructions as Fig. 2.2, and it must take extra time to arrive at the receiver. The additional propagation time is so-called the Non-Line-of-Sight (NLOS) error, and is always positive as presented in Fig. 2.1. The NLOS error is viewed as a killer issue for location estimation [12]. The excess part of the time measurements will result in range errors on the order of 513 meters and 436 meters in the mean and the standard deviation respectively [13], which inevitably makes a time-based location algorithm to fail.

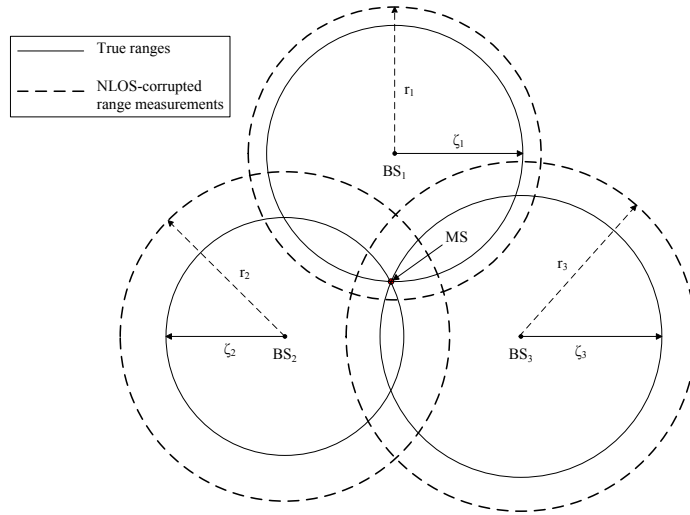


Figure 2.1: The range measurements Suffer from the NLOS errors.

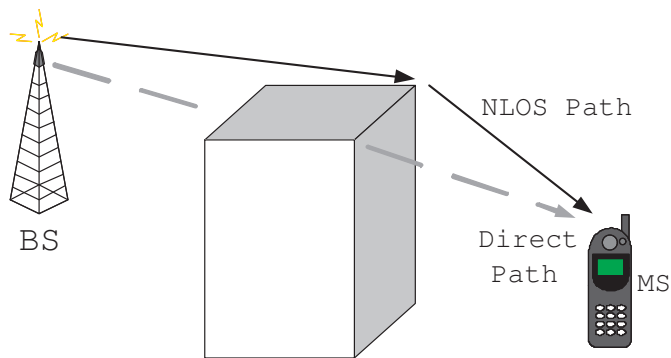


Figure 2.2: Geometry of the NLOS error

## 2.2 Studies on Existing Location Estimation Algorithms

Different location estimation schemes have been proposed to acquire the MS's position. Various types of information (e.g. the signal propagation time, the received angle of the signal, or the Receiving Signal Strength (RSS)) are involved to facilitate the algorithms design for location estimation. The primary objectives in most of the location estimation algorithms are to obtain higher estimation accuracy with promoted computational efficiency. Some famous algorithm such as range scaling algorithm (RSA), proposed in [14] to alleviate the NLOS errors by considering the geometric layout between the MS and its associated BSs. Virtual base stations (VBS) [15], mitigate the influence from the NLOS errors by imposing the geometric constraints and reduce the GDOP effect by incorporating the assisted virtual base stations. Multiple signal classification (MUSIC) [16] - [18] scheme, is experimentally illustrated to be a robust solution for location estimation, especially for a near-far environment.

There are also different approaches adopting linearized methods to acquire the computing efficiency while obtaining an approximate estimation of the MS's position. The Taylor-series estimation (TSE) method was utilized in [4] to acquire the location estimation from the TDOA measurements. The method requires iterative processes to obtain the location estimate from a linearized system. The major drawback of this method is that it may suffer from the convergence problem due to an incorrect initial guess of the MS's position. The two-step LS method was adopted to solve the location estimation problem from the TOA [20], the TDOA [5], and the TDOA/AOA measurements [21]. It is an approximate realization of the Maximum Likelihood (ML) estimator and does not require iterative processes. The two-step LS scheme is advantageous in its computational efficiency with adequate accuracy for location estimation. However, the scheme is



demonstrated to be feasible for acquiring the MS's position under the LOS situations.

Some well-known schemes are improved continuously in order to achieve higher accuracy or promote the computational efficiency. The famous linear time-based algorithms, the Taylor-series estimation (TSE) [4] and the two-step LS method are briefly described in the following subsection.

### 2.2.1 Taylor-Series Estimation

The content of this section will show the Taylor-Series Estimation (TSE), which is available in [4].

Assuming that  $(x, y)$  is the position of the MS,  $(x_\ell, y_\ell)$  is the position of the  $\ell^{\text{th}}$  base station and  $r_\ell$  is the TOA measurement from the base station  $\ell$ . Since in practice, especially in urban or in mountainous areas, the signals from the mobile device are usually unable to arrive at the base stations directly (or in the opposite direction), they always take a longer path than the direct one. So by incorporating the influences of NLOS propagation on the location estimation, there exists

$$f_\ell(x, y, x_\ell, y_\ell) = \zeta_\ell = r_\ell - n_\ell \quad (2.1)$$

where  $\zeta_\ell$  represents the noiseless distance between the MS and the  $\ell^{\text{th}}$  BS.  $n_\ell$  is the measurement noise and is statistically distributed. We take the noises to have zero-mean values  $\langle n_\ell \rangle = 0$  and  $n_{ij} = \langle n_i n_j \rangle$  is the  $i - j^{\text{th}}$  term in the covariance matrix

$$\mathbf{Q} = [n_{ij}]$$

If the  $x_v, y_v$  are guesses of the true variable position, write

$$x = x_v + \delta_x \quad y = y_v + \delta_y \quad (2.2)$$

and expand  $f_\ell$  in Taylor's series keeping only terms below second order

$$f_{\ell v} + a_{\ell 1}\delta_x + a_{\ell 2}\delta_y \simeq r_\ell - n_\ell \quad (2.3)$$

where

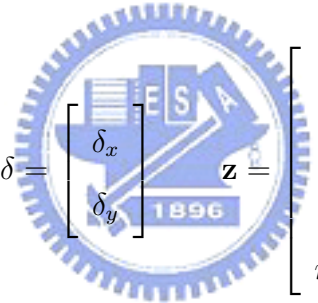
$$f_{\ell v} = f_\ell(x_v, y_v, x_\ell, y_\ell)$$

$$a_{\ell 1} = \partial f_\ell / \partial x|_{x_v, y_v} \quad a_{\ell 2} = \partial f_\ell / \partial y|_{x_v, y_v}$$

and the approximate relations of 2.3 can be written as

$$\mathbf{A}\delta \simeq \mathbf{z} - \mathbf{n} \quad (2.4)$$

where

$$\mathbf{A} = \begin{bmatrix} a_{11} & a_{12} \\ a_{21} & a_{22} \\ \cdot & \cdot \\ a_{N1} & a_{N2} \end{bmatrix} \quad \delta = \begin{bmatrix} \delta_x \\ \delta_y \end{bmatrix} \quad \mathbf{z} = \begin{bmatrix} r_1 - f_{1v} \\ r_2 - f_{2v} \\ \cdot \\ r_N - f_{Nv} \end{bmatrix} \quad \mathbf{n} = \begin{bmatrix} n_1 \\ n_2 \\ \cdot \\ n_N \end{bmatrix}$$


The choice of  $\delta$  that

$$\delta = (\mathbf{A}^T \mathbf{Q}^{-1} \mathbf{A})^{-1} \mathbf{A}^T \mathbf{Q} \mathbf{z} \quad (2.5)$$

Thus, to estimate the position of the MS, compute  $\delta_x, \delta_y$  with (2.5), replace

$$x_v \leftarrow x_v + \delta_x \quad y_v \leftarrow y_v + \delta_y \quad (2.6)$$

in (2.5), and repeat the computations. The iterations will have converged when  $\delta_x$  and

$\delta_y$  are essentially zero.

## 2.2.2 Two-Step Least Square Method

The content of this section will show the Two-step Least Square (two-step LS) location algorithm for TOA measurements and it can be obtained in [20]. For simplification, the two-step LS method will be described for TOA measurements in a two-dimensional (2-D) plane. The two-step LS method for TDOA measurements can be derived from the similar concept.

Assuming that  $(x, y)$  is the position of the mobile device,  $(x_\ell, y_\ell)$  is the position of the  $\ell^{\text{th}}$  base station and  $r_\ell$  is the TOA measurement from the base station  $\ell$ . Since in practice, especially in urban or in mountainous areas, the signals from the mobile device are usually unable to arrive at the base stations directly (or in the opposite direction), they always take a longer path than the direct one. So by incorporating the influences of NLOS propagation, killer issue for location estimation, on the location estimation, there exists

$$r_\ell^2 \geq (x_\ell - x)^2 + (y_\ell - y)^2 = \kappa_\ell - 2x_\ell x - y_\ell y + x^2 + y^2 \quad \ell = 1, 2, \dots, N \quad (2.7)$$

where  $\kappa_\ell = x_\ell^2 + y_\ell^2$ ,  $r_\ell = ct_\ell$  is the measured distance between the MS and the  $\ell$ th base station, and  $c$  is the speed of light. And by defining a new variable  $\beta = x^2 + y^2$ , we rewrite (2.7) through a set of linear expressions

$$-2x_\ell x - 2y_\ell y + \beta \leq r_\ell^2 - \kappa_\ell \quad \ell = 1, 2, \dots, N \quad (2.8)$$

Let  $\mathbf{x}_a = [x \ y \ \beta]^T$  and express (2.8) in matrix form

$$\mathbf{H}\mathbf{x}_a \leq \mathbf{J} \quad (2.9)$$

where

$$\mathbf{H} = \begin{bmatrix} -2x_1 & -2y_1 & 1 \\ -2x_2 & -2y_2 & 1 \\ \cdot & \cdot & \cdot \\ -2x_N & -2y_N & 1 \end{bmatrix} \quad \mathbf{J} = \begin{bmatrix} r_1^2 - \kappa_1 \\ r_2^2 - \kappa_2 \\ \cdot \\ r_N^2 - \kappa_N \end{bmatrix}$$

With measurement noise, the error vector is

$$\boldsymbol{\psi} = \mathbf{J} - \mathbf{H}\mathbf{x}_a \quad (2.10)$$

When  $r_\ell$  can be expressed as  $\xi_\ell + cn_\ell$ , the error vector  $\boldsymbol{\psi}$  is found to be

$$\begin{aligned} \boldsymbol{\psi} &= 2c\mathbf{B}\mathbf{n} + c^2\mathbf{n} \odot \mathbf{n} \\ \mathbf{B} &= \text{diag}\{\xi_1, \xi_2, \dots, \xi_N\} \end{aligned} \quad (2.11)$$

The symbol  $\odot$  represents the Schur product (element-by-element product). In addition, the second term on the right of (2.11) can be ignored since the condition  $cn_\ell \leq \xi_\ell$  is usually satisfied. As a result,  $\boldsymbol{\psi}$  becomes a Gaussian random vector with covariance matrix given by

$$\boldsymbol{\Psi} = E[\boldsymbol{\psi}\boldsymbol{\psi}^T] = 4c^2\mathbf{B}\mathbf{Q}\mathbf{B} \quad (2.12)$$

$\mathbf{Q}$  is the covariance matrix of measured noise, and  $\xi_1, \dots, \xi_N$  are denoted as the true values of distances between the sources and the receiver. The element  $\mathbf{x}_a$  are related by the equation,  $\beta = x^2 + y^2$ , which means that (2.9) is still a set of nonlinear equations in two variables  $x$  and  $y$ . The approach to solve the nonlinear problem is to first assume that there is no relationship among  $x$ ,  $y$  and  $\beta$ . That can then be solved by Least Square (LS). The final solution is obtained by imposing the known relationship to the computed result via another LS computation. This two step procedure is an approximation of a true ML

estimator. By considering the elements of  $\mathbf{x}_a$  independent, the ML estimator of  $\mathbf{x}_a$  is

$$\begin{aligned}\mathbf{x}_a &= \arg \min\{(\mathbf{J} - \mathbf{H}\mathbf{x})^T \Psi^{-1}(\mathbf{J} - \mathbf{H}\mathbf{x})\} \\ &= (\mathbf{H}^T \Psi^{-1} \mathbf{H})^{-1} \mathbf{H}^T \Psi^{-1} \mathbf{J}\end{aligned}\quad (2.13)$$

The covariance matrix of  $\mathbf{x}_a$  is obtained by evaluating the expectations of  $\mathbf{x}_a$  and  $\mathbf{x}_a \mathbf{x}_a^T$  from (2.13). The covariance matrix of  $\mathbf{x}_a$  can be calculated as [?]

$$\text{cov}(\mathbf{x}_a) = (\mathbf{H}^T \Psi^{-1} \mathbf{H})^{-1} \quad (2.14)$$

Since we have used the independent supposition of variables  $x$ ,  $y$ , and  $\beta$  in the estimation of  $\mathbf{x}_a$  though the variable  $\beta$  is dependent on the variable  $x$  and  $y$ , we should revise the results as follows. Let the estimation errors of  $x$ ,  $y$ , and  $\beta$  be  $e_1$ ,  $e_2$ , and  $e_3$ . Here and below, denote the  $i^{\text{th}}$  entry of a matrix  $M$  as  $[M]_i$ ; then the entries in vector  $\mathbf{x}_a$  become

$$[\mathbf{x}_a]_1 = x_o + e_1 \quad (2.15a)$$

$$[\mathbf{x}_a]_2 = y_o + e_2 \quad (2.15b)$$

$$[\mathbf{x}_a]_3 = \beta_o + e_3 \quad (2.15c)$$

where  $x_o$ ,  $y_o$ , and  $\beta_o$  are denoted as the true values of  $x$ ,  $y$ , and  $\beta$ . Let another error vector

$$\psi_b = \mathbf{J}_b - \mathbf{H}_b \mathbf{x}_b \quad (2.16)$$

where

$$\mathbf{H}_b = \begin{bmatrix} 1 & 0 \\ 0 & 1 \\ 1 & 1 \end{bmatrix} \quad \mathbf{J}_b = \begin{bmatrix} [\mathbf{x}_a]_1^2 \\ [\mathbf{x}_a]_2^2 \\ [\mathbf{x}_a]_3 \end{bmatrix}$$

and  $\mathbf{x}_b = \begin{bmatrix} x^2 \\ y^2 \end{bmatrix}$ . Substituting 2.15a- 2.15c into 2.16, we have

$$[\psi]_1 = 2x_o e_1 + e_1^2 \approx 2x_o e_1$$

$$[\psi]_2 = 2y_o e_2 + e_2^2 \approx 2y_o e_2$$

$$[\psi]_3 = e_3$$

Obviously, the above approximations are valid only when the errors  $e_1$ ,  $e_2$ , and  $e_3$  are fairly small. Subsequently, the covariance matrix of  $\psi_b$  is

$$\begin{aligned} \Psi_b &= E[\psi_b \psi_b^T] = 4\mathbf{B}_b \text{cov}(\mathbf{x}) \mathbf{B}_b \\ \mathbf{B}_b &= \text{diag}\{x_o, y_o, 0.5\} \end{aligned} \quad (2.18)$$

As an approximation, elements  $x_o$  and  $y_o$  in matrix  $\mathbf{x}$  can be replaced by the first two elements  $x$  and  $y$  in  $\mathbf{x}_a$ . Similarly, the ML estimate of  $\mathbf{x}_b$  is given by

$$\mathbf{x}_b = (\mathbf{H}_b^T \Psi_b^{-1} \mathbf{H}_b)^{-1} \mathbf{H}_b^T \Psi_b^{-1} \mathbf{J}_b \quad (2.19)$$

$$\approx (\mathbf{H}_b^T \mathbf{B}_b^{-1} (\text{cov}(\mathbf{x})_a)^{-1} \mathbf{B}_b^{-1} \mathbf{H}_b)^{-1} \quad (2.20)$$

$$\bullet (\mathbf{H}_b^T \mathbf{B}_b^{-1} (\text{cov}(\mathbf{x})_a)^{-1} \mathbf{B}_b^{-1}) \mathbf{J}_b \quad (2.21)$$

So the final position estimation  $\mathbf{x} = [x \quad y]^T$  is

$$\mathbf{x} = \sqrt{\mathbf{x}_b}, \quad \text{or} \quad \mathbf{x} = -\sqrt{\mathbf{x}_b} \quad (2.22)$$

Here the sign of  $x$  should coincide with the sign of  $[\mathbf{x}_a]_1$  calculated by solving 2.13, and the sign of  $y$  coincides with the sign of  $[\mathbf{x}_a]_2$ .

The complete derivation of the two-step LS for TOA measurements is shown above. In

addition, the two-step LS method can be adopted to estimate MS location from the TDOA [5], and the TDOA/AOA measurements [21]. The following two subsections describe the 3-D TOA location estimation for the satellite-based system, and the 3-D TDOA/AOA location estimation algorithm for the cellular network.

### 2.2.3 Geometry-Constrained Location Estimation (GLE) Algorithm

Sveral location algorithms [22]- [26] have been proposed to mitigate the NLOS error. Here we introduce a method by using the geometric property. As illustrated in Fig. 2.3 , the MS's location estimation using the two-step LS method may fall inside or outside of the boundaries of the three arcs, **AB**, **BC**, and **CA**. With the larger overlap region caused by the increasing NLOS error, the inaccuracy of the location estimation of the MS consequentially raises. The characteristics of the geometric layout and the noise variances are applied to a method named the Geometry-Constrained Location Estimation (GLE) algorithm [27] to modify the formulations within the Two-Step Least Square method. The primary objective of the proposed GLE algorithm is to confirm the location estimate within the overlap region by joining the geometric constraints into the Two-Step LS method.

A specific information derived from the constraints of the geometric layout is added into the Two-Step Least Square method. The constrained cost function  $\gamma$  is given by

$$\gamma = \left[ \sum_{\mu=\mathbf{a},\mathbf{b},\mathbf{c}} \frac{1}{3} \|\mathbf{x} - \mu\|^2 \right]^{1/2} \quad (2.23)$$

where  $\mathbf{x}$  is the MS's location as mentioned before;  $\mathbf{a} = (x_a, y_a)$ ,  $\mathbf{b} = (x_b, y_b)$ , and  $\mathbf{c} = (x_c, y_c)$  represent the corresponding coordinates of the points  $A$ ,  $B$ , and  $C$ . The parameter  $\gamma$  defined as the square root of the average squared-sum of the distance from the MS to the

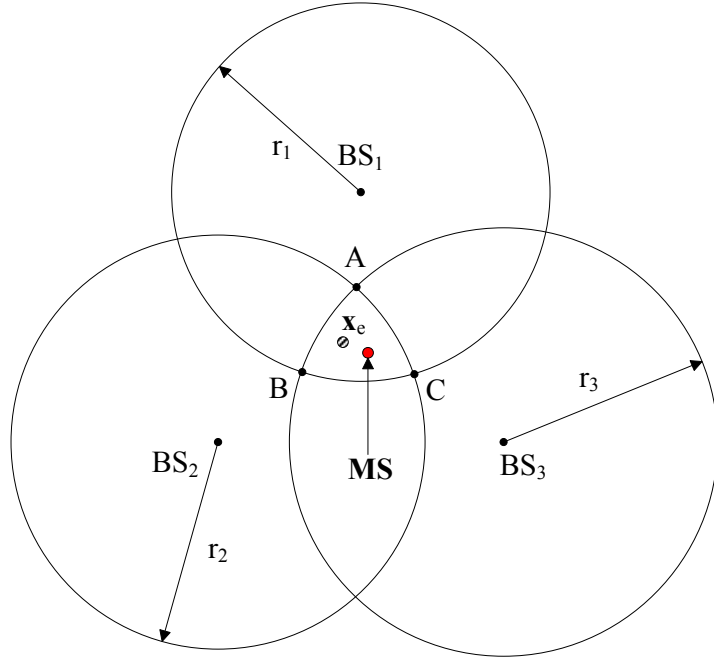


Figure 2.3: Geometric constraints for TOA-Based location estimation confine the true MS's position in the overlap region of the range measurements.

three points **A**, **B** and **C** is called the *virtual distance* and obviously varies as the three coordinates **a**, **b** and **c** changes. The corresponding *expected virtual distance*  $\gamma_e$  is defined as

$$\gamma_e = \left[ \sum_{\mu=\mathbf{a},\mathbf{b},\mathbf{c}} \frac{1}{3} \|\mathbf{x}_e - \mu\|^2 \right]^{1/2} = \gamma + n_\gamma \quad (2.24)$$

where  $n_\gamma$  is the error induced by the computed deviation between  $\gamma_e$  and  $\gamma$ . The  $\mathbf{x}_e$  called the expected MS's position is chosen to minimize the deviation between the *virtual distance*  $\gamma$  and the corresponding *expected virtual distance*  $\gamma_e$ . The coordinates of the expected MS position  $\mathbf{x}_e$  is a linear combination of those of the three points **A**, **B**, and **C**



with the parameters acting as weights which is related to the signal variations.

$$x_e = w_1x_a + w_2x_b + w_3x_c \quad (2.25a)$$

$$y_e = w_1y_a + w_2y_b + w_3y_c \quad (2.25b)$$

where

$$w_\ell = \frac{\sigma_\ell^2}{\sigma_1^2 + \sigma_2^2 + \sigma_3^2} \quad \text{for } \ell = 1, 2, 3 \quad (2.26)$$

$\sigma_1$ ,  $\sigma_2$ , and  $\sigma_3$  are the corresponding standard deviations obtained from the three TOA measurements  $r_1$ ,  $r_2$ , and  $r_3$ .

The selection of the weights is directly proportional to the corresponding signal variances. For example, the excessive range measurement  $r_1$  due to the comparatively large signal variance  $\sigma_1$  may probably cause the true position of the MS to move incorrectly toward to the boundary of the arc **BC**. Therefore, the weighting of the coordinates of  $\mathbf{a}$  should be relatively large to make the true position of the MS to move toward the point A of the analogous triangle.

The GLE algorithm integrates the geometric constraints into the first step of the Two-Step Least Square method is defined as:

$$\mathbf{H}\mathbf{x} = \mathbf{J} + \psi \quad (2.27)$$

where

$$\mathbf{x} = \begin{bmatrix} x & y & \beta \end{bmatrix}^T$$

$$\mathbf{H} = \begin{bmatrix} -2x_1 & -2y_1 & 1 \\ -2x_2 & -2y_2 & 1 \\ -2x_3 & -2y_3 & 1 \\ -2\gamma_x & -2\gamma_y & 1 \end{bmatrix}$$

$$\mathbf{J} = \begin{bmatrix} r_1^2 - \kappa_1 \\ r_2^2 - \kappa_2 \\ r_3^2 - \kappa_3 \\ \gamma_e^2 - \gamma_\kappa \end{bmatrix}$$

The corresponding coefficients are given by

$$\beta = x^2 + y^2$$

$$\kappa_\ell = x_\ell^2 + y_\ell^2 \quad \text{for } \ell = 1, 2, 3$$

$$\gamma_x = \frac{1}{3}(x_a + x_b + x_c)$$

$$\gamma_y = \frac{1}{3}(y_a + y_b + y_c)$$

$$\gamma_\kappa = \frac{1}{3}(x_a^2 + x_b^2 + x_c^2 + y_a^2 + y_b^2 + y_c^2)$$

The noise matrix  $\psi$  in (2.27) can be obtained as

$$\psi = 2c \mathbf{B} \mathbf{n} + c^2 \mathbf{n}^2 \quad (2.28)$$

where

$$\mathbf{B} = \text{diag} \left\{ \zeta_1, \zeta_2, \zeta_3, \gamma \right\}$$

$$\mathbf{n} = \left[ n_1 \quad n_2 \quad n_3 \quad n_\gamma/c \right]^T$$

Based on the two-step LS scheme, an intermediate location estimate after the first step

can be obtained as

$$\hat{\mathbf{x}} = (\mathbf{H}^T \mathbf{\Psi}^{-1} \mathbf{H})^{-1} \mathbf{H}^T \mathbf{\Psi}^{-1} \mathbf{J} \quad (2.29)$$

where

$$\mathbf{\Psi} = E[\psi\psi^T] = 4 c^2 \mathbf{BQB}$$

It is noted that  $\mathbf{\Psi}$  is obtained by neglecting the second term of (2.28). The matrix  $\mathbf{Q}$  can be acquired as

$$\mathbf{Q} = \text{diag} \left\{ \sigma_1^2, \sigma_2^2, \sigma_3^2, \sigma_{\gamma_e/c}^2 \right\}$$

$\mathbf{Q}$  represents the covariance matrix for both the TOA measurements and the *expected virtual distance*, where  $\sigma_{\gamma_e/c}^2$  corresponds to the standard deviation of  $\gamma_e/c$ . The final location estimation can be obtained by continuously carrying on the second step of the Two-Step Least Square method [20].



# Chapter 3

## Derivation from GDOP and GDOP

### MOM Metric

The time-based algorithms, i.e. TSE and two-step LS as described in chapter 2, are primarily feasible for location estimation under line-of-sight (LOS) environments. As described in chapter2, NLOS error is an important issue for Wireless Location System. In order to preserve the computation efficiency and to obtain higher accuracy under NLOS environments, geometric constraints are added to enhance the existing algorithm. Two geometry metric, geometric dilution of precision (GDOP) and GDOP measure-of-merit(MOM), are proposed in this chapter and some properties will be derived for company. We'll introduce these two mathematical metrics at section 3.1 and 3.2 and derive some properties at section 3.1.1 and 3.1.2.

### 3.1 Mathematical Modeling

The signal model for the TOA measurements is utilized in this paper. The set  $\mathbf{r}_k$  contains all the available measured relative distance at the  $k$ th time step, i.e.  $\mathbf{r}_k = \{r_{1,k}, \dots, r_{i,k}, \dots, r_{N_k,k}\}$ , where  $N_k$  denotes the number of available BSs at the time step

$k$ . The measured relative distance ( $r_{i,k}$ ) between the MS and the  $i$ th BS (obtained at the  $k$ th time step) can be represented as

$$r_{i,k} = c \cdot t_{i,k} = \zeta_{i,k} + n_{i,k} + e_{i,k} \quad i = 1, 2, \dots, N_k \quad (3.1)$$

where  $t_{i,k}$  denotes the TOA measurement obtained from the  $i$ th BS at the  $k$ th time step, and  $c$  is the speed of light.  $r_{i,k}$  is contaminated with the TOA measurement noise  $n_{i,k}$  and the NLOS error  $e_{i,k}$ . It is noted that the measurement noise  $n_{i,k}$  is in general considered as zero mean with Gaussian distribution. On the other hand, the NLOS error  $e_{i,k}$  is modeled as exponentially-distributed for representing the positive bias due to the non-line-of-sight effect [22]. The noiseless relative distance  $\zeta_{i,k}$  (in (3.1)) between the MS's true position and the  $i$ th BS can be obtained as

$$\zeta_{i,k} = [(x_k - x_{i,k})^2 + (y_k - y_{i,k})^2]^{\frac{1}{2}} \quad (3.2)$$

where  $\mathbf{x}_k = [x_k \ y_k]$  represents the MS's true position and  $\mathbf{x}_{i,k} = [x_{i,k} \ y_{i,k}]$  is the location of the  $i$ th BS for  $i = 1$  to  $N_k$ . Therefore, the set of all the available BSs at the  $k$ th time step can be obtained as  $\mathbf{P}_{BS,k} = \{\mathbf{x}_{1,k}, \dots, \mathbf{x}_{i,k}, \dots, \mathbf{x}_{N_k,k}\}$ .

The architecture can be described as Fig. 3.1. After getting the information as describe above, the next step is solving the MS position. The object's position can be represent by a n-dimensional vector  $\mathbf{h}$ .  $\mathbf{h} = [x_k \ y_k]^T$  in 2-D space. However, before we continue and introduce the geometry for specific bearing measurements, we will state some results from estimation theory.

$$Z_i = f_i(\mathbf{h}) + N_i \quad i = 1, 2, \dots \quad (3.3)$$

where  $N_i \sim N(0, \sigma_i^2)$  for zero mean Gaussian noise.

A major problem is to solve the nonlinear system of equations. So a first step is

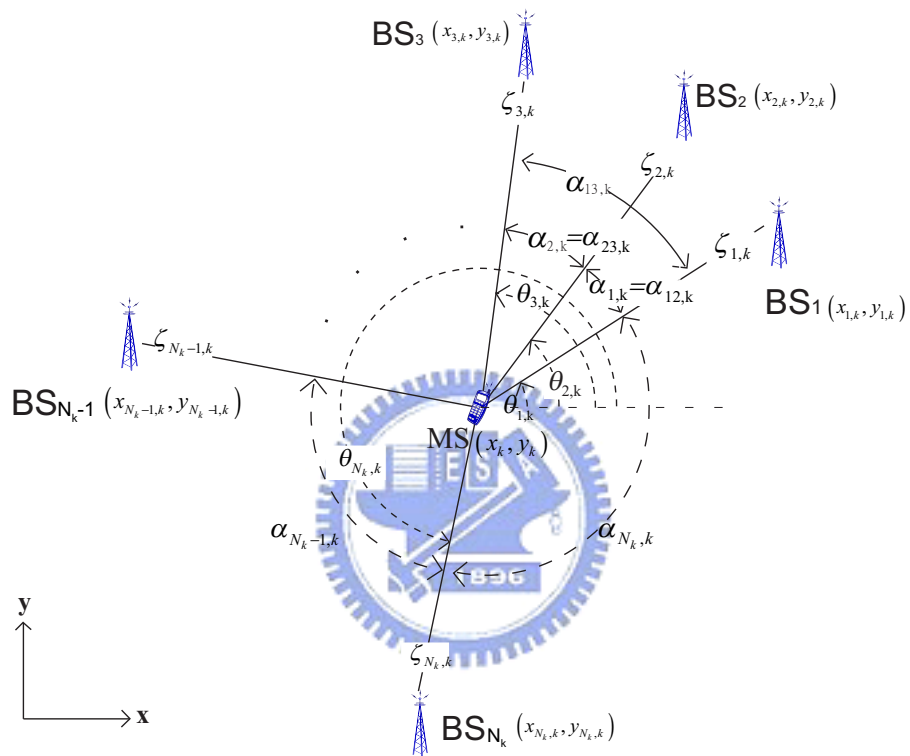


Figure 3.1: Schematic diagram of the network layout for computation.

linearization. It can be achieved by using Taylor series expansion.

$$f(\tilde{h}) = \sum_{i=0}^n \frac{f^i(v)}{i!} (\tilde{h} - v)^i \quad (3.4)$$

If we take first order approximation and let  $\tilde{x}$  be the accurate position, equation can be written as  $f(\tilde{h}) \approx f(\tilde{x}) + H \cdot (\tilde{h} - \tilde{x})$ . As described above, it can be functionally related as  $df = H \cdot dx + e$  Where  $e$  means the high order term error. The LS solution is given by:

$$dx = (H^T H)^{-1} H^T df \quad (3.5)$$

The covariance of the vector  $dx$  can be obtained as

$$\begin{aligned} cov(dx) &= E[dx dx^T] \\ &= (H^T H)^{-1} H^T cov(df) ((H^T H)^{-1} H^T)^T \end{aligned} \quad (3.6)$$

In ideal case,  $cov(df) = I_2 \sigma_i^2$  where  $I_2$  is an  $2 \times 2$  identity matrix, we have

$$\begin{aligned} cov(dx) &= (H^T H)^{-1} H^T H (H^T H)^{-1} I_2 \sigma_i^2 \\ &= (H^T H)^{-1} \sigma_i^2 \end{aligned} \quad (3.7)$$

For a i.i.d. range error of covariance  $cov(df) = C_k \cdot \sigma_k$ , where  $C_k$  is a symmetric positive definite matrix and  $\sigma_k$  is the user equivalent range error variance.  $cov(dx)$  can be expressed as

$$cov(dx) = \begin{bmatrix} \sigma_{xx} & \cdot \\ \cdot & \sigma_{yy} \end{bmatrix} \quad (3.8)$$

and the off-diagonal entries are not critical to the following discussion. The most commonly used measure of the positioning accuracy is the root mean square error metric. We want to show the influence of the geometric property on the positioning accuracy. To do so, we need a metric, which describes a quality of the measurement units geometric configuration. The matrix, GDOP and GDOP MOM, can be used to evaluate the geometric layout.

### 3.2 Geometric Dilution of Precision (GDOP)

GDOP metric is utilized to describe the geometric effect on the relationship between the measurement error and the position determination error [8] [10]. Fig.3.1 illustrates the schematic diagram of the network layout for the GDOP computation. In general, a larger GDOP value corresponds to a comparably worse geometric layout (established by the MS and its associated BSs), which consequently results in augmented errors for location estimation. On the other hand, as the GDOP value becomes smaller, the effect from the geometric relationship to the location estimation accuracy will turn out to be insignificant. Considering the MS's location under the two-dimensional coordinate, the GDOP value (G) obtained at the MS's true position  $\mathbf{x}_k$  can be represented as

$$G_{\mathbf{x}_k} = \left\{ \text{trace} \left[ (\mathbf{H}_{\mathbf{x}_k}^T \mathbf{H}_{\mathbf{x}_k})^{-1} \right] \right\}^{\frac{1}{2}} \quad (3.9)$$

For measurement model in GDOP, the signal  $f(x)$  can be described as  $f(x) = \zeta_{i,k}$ . Thus the matrix  $\mathbf{H}_{\mathbf{x}_k}$  can be modeled as



$$\mathbf{H}_{\mathbf{x}_k} = \begin{bmatrix} \frac{x_k - x_{1,k}}{\zeta_{1,k}} & \frac{y_k - y_{1,k}}{\zeta_{1,k}} \\ \dots & \dots \\ \frac{x_k - x_{i,k}}{\zeta_{i,k}} & \frac{y_k - y_{i,k}}{\zeta_{i,k}} \\ \dots & \dots \\ \frac{x_k - x_{N_k,k}}{\zeta_{N_k,k}} & \frac{y_k - y_{N_k,k}}{\zeta_{N_k,k}} \end{bmatrix} \quad (3.10)$$

It is noted that the elements within the matrix  $\mathbf{H}_{\mathbf{x}_k}$  can be acquired from (3.2).

### 3.2.1 Derived GDOP property

It is noted that (3.9) associated with (3.10) are utilized for representing the GDOP metric in most of the research studies. In order to facilitate the design of the proposed GALE schemes, several properties obtained from the GDOP metrics are observed and derived in this paper. As shown in Fig. 3.1, the following relationship can be obtained with coordinate transformation as  $\mathbf{x}_k - \mathbf{x}_{i,k} = [\zeta_{i,k} \cos \theta_{i,k}, \zeta_{i,k} \sin \theta_{i,k}]$  for  $i = 1$  to  $N_k$ , where  $\theta_{i,k}$  represents the angle formed by the vector of  $\mathbf{x}_k - \mathbf{x}_{i,k}$  w.r.t. the positive  $x$ -axis. By substituting this equation into (3.10), the GDOP value in (3.9) can be rewritten as

$$G_{\mathbf{x}_k} = \left[ \frac{N_k}{\sum_{i=2}^{N_k} \sin^2(\theta_{i,k} - \theta_{i-1,k}) + \sin^2(\theta_{1,k} - \theta_{N_k,k})} \right]^{\frac{1}{2}} \quad (3.11)$$

Furthermore, in order to facilitate the proofs of the following lemmas, the relative angles  $\alpha_{i,k}$  between the BSs are defined as

$$\alpha_{i,k} = \begin{cases} \theta_{i+1,k} - \theta_{i,k} & 1 \leq i \leq N_k - 1 \\ 2\pi + \theta_{1,k} - \theta_{N_k,k} & i = 0, N_k \end{cases} \quad (3.12)$$

It is noted that  $i = 0$  is utilized for circular counting in order to facilitate the notations

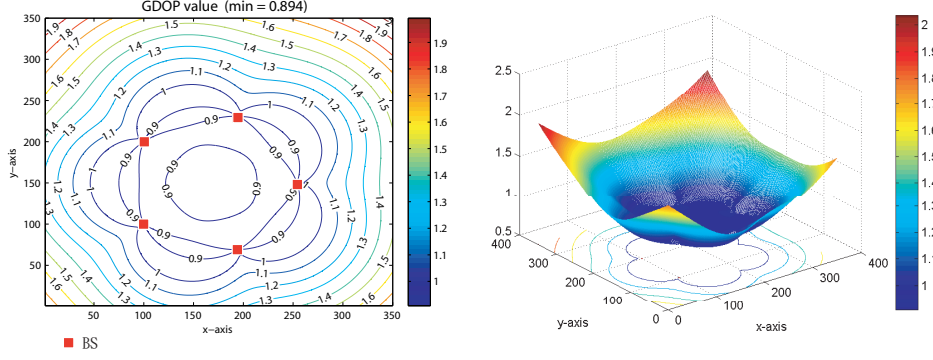


Figure 3.2: GDOP value in a regular pentagon

that will be utilized in the paper. Furthermore, the relative angles  $\alpha_{pq,k}$  between each arbitrary  $p$ th and  $q$ th BSs are further defined as

$$\alpha_{pq,k} = \begin{cases} \sum_{\forall p}^{q-1} \alpha_{p,k} & \forall p < q \\ 2\pi - \sum_{\forall q}^{p-1} \alpha_{q,k} & \forall p > q \end{cases} \quad (3.13)$$

where  $1 \leq p < N_k$ ,  $1 \leq q \leq N_k$  and  $\alpha_{p,k}$  is defined as in (3.12). Consequently, the GDOP value in (3.11) can be reformulated as a function of  $\alpha_{i,k}$  as

$$G_{x_k} = \left[ \frac{N_k}{\sum_{i=1}^{N_k-1} \sum_{j=i+1}^{N_k} \sin^2(\alpha_{ij,k})} \right]^{\frac{1}{2}} \quad (3.14)$$

The GDOP is utilized as an index for judging the the effect of the geometric layout. Several K-side regular polygon layouts are examined to verify the phenomenons of the GDOP. The 3-D graph and the contour of the GDOP value are shown in Fig. (3.2)-(3.3). The Figs. shows that when all the BSs form a regular polygon, the minimum GDOP value will occur at the center of these BSs. And we can get another observation that when MS is situated inside the polygon will have lower GDOP that outside.

In the following, the minimal GDOP values are obtained by considering two different cases. The minimal GDOP values are determined by adjusting one BS's location in

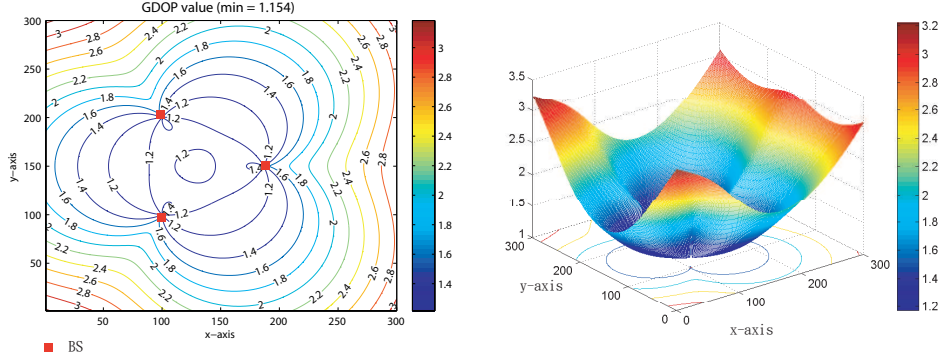


Figure 3.3: GDOP value in a regular triangle

Lemma 1 (i.e. with one degree-of-freedom) and regulating all the locations of the BSs in Lemma 2 (i.e. with  $N_k$  degree-of-freedom). The claims and derivations for both lemmas are stated as follows.

**Lemma 1.** *The MS located at  $\mathbf{x}_k$  is surrounded by  $N_k$  BSs at  $\mathbf{x}_{i,k}$  (for  $i = 1$  to  $N_k$ ) as shown in Fig. 3.1. The angles between every two adjacent BSs to the MS are defined as  $\alpha_{i,k}$ . It is assumed that only the  $\ell$ th BS's location is adjustable; i.e. the angle  $\alpha_{\ell,k}$  between the  $\ell$ th and the  $(\ell + 1)$ th BSs; while the positions for the other BSs are considered fixed. The minimal attainable GDOP occurs as the angle  $\alpha_{\ell,k}$  is adjusted to be*

$$\alpha_{\ell,k}^m = \frac{1}{2} \tan^{-1} \left( \frac{-\sin(2 \sum_{i=1, i \neq \ell-1, \ell}^{N_k} \alpha_{li,k})}{\cos(2 \sum_{i=1, i \neq \ell-1, \ell}^{N_k} \alpha_{li,k}) + 1} \right) \quad (3.15)$$

Therefore, the minimal attainable GDOP value w.r.t.  $\mathbf{x}_k$  becomes

$$G_{\mathbf{x}_k}^m = \left[ \frac{N_k}{\sin^2(\alpha_{\ell,k}^m) + \sin^2(2\pi - \alpha_{\ell,k}^m - \sum_{i=1, i \neq \ell-1, \ell}^{N_k} \alpha_{li,k}) + \sum_{i=1, i \neq \ell-1, \ell}^{N_k} \sin^2(\alpha_{li,k})} \right]^{\frac{1}{2}} \quad (3.16)$$

*Proof.* According to (3.14), it is observed that the GDOP value  $G_{\mathbf{x}_k}$  w.r.t.  $\mathbf{x}_k$  is regarded as a function of the angles  $\alpha_{i,k}$  for all  $i = 1$  to  $N_k$ . Since only the  $\ell$ th BS (for  $1 \leq \ell \leq N_k$ ) is considered adjustable, there is merely one degree-of-freedom that is considered tunable (i.e.  $\alpha_{\ell,k}$ ) among all the angles  $\alpha_{i,k}$  for  $i = 1$  to  $N_k$ . It is noted that the other angle

$\alpha_{\ell-1,k}$ , which is also modified due to the movement of the  $\ell$ th BS, can be represented as a function of  $\alpha_{\ell,k}$ , i.e.  $\alpha_{\ell-1,k} = 2\pi - \alpha_{\ell,k} - \sum_{i=1, i \neq \ell-1, \ell}^{N_k} \alpha_{i,k}$ . Consequently, the GDOP value as denoted in (3.14) will only be dependent to the angle  $\alpha_{\ell,k}$  as  $G_{\mathbf{x}_k}(\alpha_{\ell,k})$ . The angle  $\alpha_{\ell,k}^m$  which results in the minimal GDOP value can therefore be acquired as

$$\alpha_{\ell,k}^m = \arg \left\{ \min_{\forall \alpha_{\ell,k}} G_{\mathbf{x}_k}(\alpha_{\ell,k}) \right\} \quad (3.17)$$

It can be observed that (3.32) can be achieved if the following conditions on the first and second derivatives of  $G_{\mathbf{x}_k}$  are satisfied, i.e.

$$\left[ \frac{\partial G_{\mathbf{x}_k}(\alpha_{\ell,k})}{\partial \alpha_{\ell,k}} \right]_{\alpha_{\ell,k} = \alpha_{\ell,k}^m} = 0 \quad (3.18)$$

$$\left[ \frac{\partial^2 G_{\mathbf{x}_k}(\alpha_{\ell,k})}{\partial^2 \alpha_{\ell,k}} \right]_{\alpha_{\ell,k} = \alpha_{\ell,k}^m} > 0 \quad (3.19)$$

By solving (3.33) and (3.34), the angle  $\alpha_{\ell,k}^m$  can be computed as in (3.15). The minimal GDOP value w.r.t.  $\mathbf{x}_k$  can consequently be obtained as in (3.16).  $\square$

**Lemma 2.** *The MS located at  $\mathbf{x}_k$  is surrounded by  $N_k$  BSs at  $\mathbf{x}_{i,k}$  (for  $i = 1$  to  $N_k$ ) as shown in Fig. 3.1. The angles between every two adjacent BSs to the MS are defined as  $\alpha_{i,k}$ . Considering the case that the locations of all the BSs are adjustable. The minimal GDOP value w.r.t.  $\mathbf{x}_k$  is obtained as  $G_{\mathbf{x}_k}^m = 2/\sqrt{N_k}$ , which occurs as the angles  $\alpha_{i,k}$  are regulated to be equivalent with each other as  $\alpha_{i,k}^m = 2\pi/N_k$  for all  $i = 1$  to  $N_k$ .*

*Proof.* It can be observed from (3.14) that the GDOP value is regarded as a function of the angles  $\alpha_{i,k}$  for all  $i = 1$  to  $N_k$ , i.e.  $G_{\mathbf{x}_k}(\alpha_{1,k}, \dots, \alpha_{i,k}, \dots, \alpha_{N_k,k})$ . By defining  $\boldsymbol{\alpha}_k = [\alpha_{1,k} \dots \alpha_{i,k} \dots \alpha_{N_k,k}]$ , the angles  $\alpha_{i,k}^m$  which result in the minimal GDOP value can

therefore be acquired as

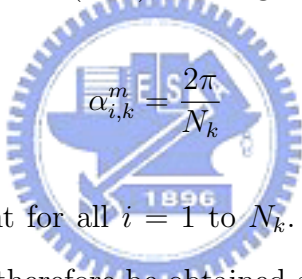
$$\alpha_{i,k}^m = \arg \left\{ \min_{\forall \alpha_{i,k}} G_{\mathbf{x}_k}(\boldsymbol{\alpha}_k) \right\} \quad (3.20)$$

for  $i = 1$  to  $N_k$ . Similar to the proof as in Lemma 1,  $\alpha_{i,k}^m$  in (3.35) can be acquired if

$$\left[ \frac{\partial G_{\mathbf{x}_k}(\boldsymbol{\alpha}_k)}{\partial \alpha_{i,k}} \right]_{\boldsymbol{\alpha}_k = \boldsymbol{\alpha}_k^m} = 0 \quad (3.21)$$

$$\left[ \frac{\partial^2 G_{\mathbf{x}_k}(\boldsymbol{\alpha}_k)}{\partial^2 \alpha_{i,k}} \right]_{\boldsymbol{\alpha}_k = \boldsymbol{\alpha}_k^m} > 0 \quad (3.22)$$

for  $i = 1$  to  $N_k$ . It is noted that  $\boldsymbol{\alpha}_k^m \triangleq [\alpha_{1,k}^m \dots \alpha_{i,k}^m \dots \alpha_{N_k,k}^m]$ . By solving the set of  $2N_k$  equations obtained from (3.21) and (3.22), the angles  $\alpha_{i,k}^m$  can be computed as

$$\alpha_{i,k}^m = \frac{2\pi}{N_k} \quad (3.23)$$


which are considered equivalent for all  $i = 1$  to  $N_k$ . By substituting (3.23) into (3.14), the minimal GDOP value can therefore be obtained as

$$G_{\mathbf{x}_k}^m(\boldsymbol{\alpha}_k^m) = \frac{2}{\sqrt{N_k}} \quad (3.24)$$

□

which occurs as the angles  $\alpha_{i,k}$  are regulated to be equivalent with each other as  $\alpha_{i,k}^m = 2\pi/N_k$

**Corollary 1.** *Considering the MS is confined by an  $N_k$ -side regular polygon by placing the  $N_k$  BSs as the vertices of the polygon, the minimal GDOP value w.r.t.  $\mathbf{x}_k$  will occur at the center of the regular polygon.*

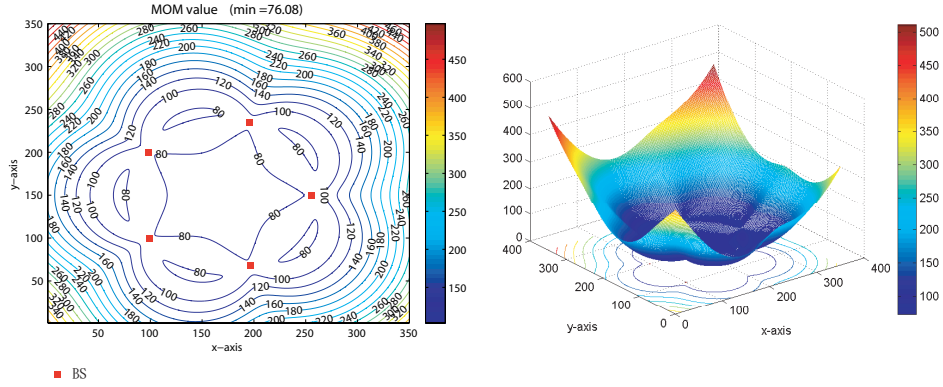


Figure 3.4: MOM value in a regular pentagon

*Proof.* This corollary is considered as a special case of Lemma 2 with all the relative distances  $\zeta_{i,k}$  are equal for  $i = 1$  to  $N_k$ . It is observed from (3.14) that the GDOP value  $G_{x_k}$  is unrelated to the relative distances  $\zeta_{i,k}$ . Therefore, the proof as presented in Lemma 2, can be carried directly to this case as obtained by (3.23) and (3.24). Therefore, it is intuitive to observe that the minimal GDOP will happen at the center point of the  $N_k$ -side regular polygon based on the result that  $\alpha_{i,k}^m = 2\pi/N_k$  for  $i = 1$  to  $N_k$ .  $\square$

### 3.3 GDOP Measure-of-Merit (MOM)

Another relative geometry measure-of-merit (MOM) [9], based on the GDOP measure, is developed. The GDOP MOM relates the BS measurement errors to the MS position errors as a function of BS-to-MS geometry. The minimum GDOP and associated specific BS-to-MS geometries are computed and illustrated for both two and three bearing-only measuring sensors. Two different polygon fig.3.4 and fig.3.5 plots of MOM value contours provide a geometric insight to BSs arrangement as a function of geometry induced error dilution. The results can be used to select preferred target-to-sensor(s) geometries for M BSs in this application.

In order to establish the necessary mathematical framework for the computation of the MOM, it is structured as follows. A linearized measurement model-based error sensitivity

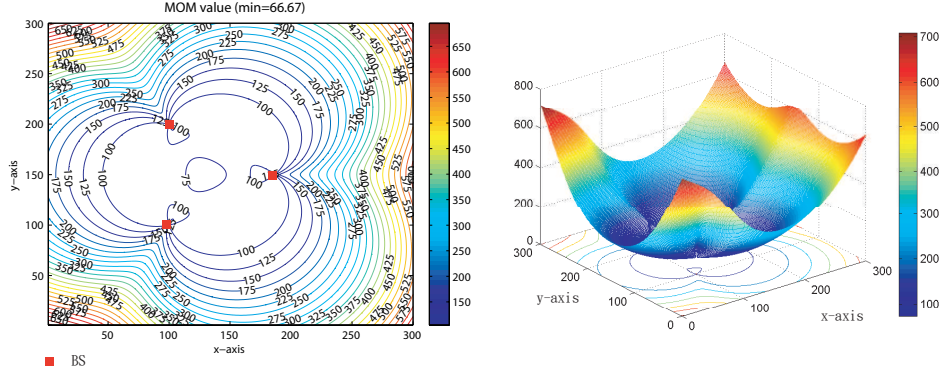


Figure 3.5: MOM value in a regular triangle

analysis is used to derive an express for the MOM. The MOM relates the measurement errors to the MS position errors as a function of BS-MS geometry. In order to illustrate the efficacy of MOM for fusion architectures, GDOP functional relationships are next computed for measuring geometry. The minimum MOM and associated specific BS-MS geometries are computed and illustrated and provide a geometric insight to BS placement as a function of geometry induced error dilution. The MOM is general and is readily extendable to other measurement based system.

The same procedure as the derivation above, MOM defines the measurement signal  $f(x) = \theta_{i,k}$  where  $\theta_{i,k}$  is the angel between the line connected MS with BS and the horizontal and can be presented as:

$$\theta_{i,k} = \tan^{-1}\left(\frac{y_{i,k} - y_k}{x_{i,k} - x_k}\right) \quad (3.25)$$

Proceeding in an analogous manner to the development of GDOP, the matrix  $\mathbf{MH}_{x_k}$  can be modeled as

$$\mathbf{MH}_{\mathbf{x}_k} = \begin{bmatrix} -\frac{y_k - y_{1,k}}{\zeta_{1,k}^2} & \frac{x_k - x_{1,k}}{\zeta_{1,k}^2} \\ \dots & \dots \\ -\frac{y_k - y_{i,k}}{\zeta_{i,k}^2} & \frac{x_k - x_{i,k}}{\zeta_{i,k}^2} \\ \dots & \dots \\ -\frac{y_k - y_{N_k,k}}{\zeta_{N_k,k}^2} & \frac{x_k - x_{N_k,k}}{\zeta_{N_k,k}^2} \end{bmatrix} \quad (3.26)$$

and MOM value  $\text{MG}_{\mathbf{x}_k}$  can be obtained as

$$\text{MG}_{\mathbf{x}_k} = \left\{ \text{trace} \left[ (\mathbf{MH}_{\mathbf{x}_k}^T \mathbf{MH}_{\mathbf{x}_k})^{-1} \right] \right\}^{\frac{1}{2}} \quad (3.27)$$

### 3.3.1 Derived MOM property

The MOM criterion is used in the location system to check if the layout of the BS is good for the goal of positioning, and it can be applied to the wireless location system as well. The interpretation of the meaning of the MOM is that it represents the standard deviation ratio of the signal and the noise. In a fixed layout, the signal variations differ with where the MS locates. The radio signals range over larger variations not only raise the inaccuracy of the location estimation but also the value of the MOM. In other words, the lower value of the MOM stands for the smaller signal variations in a fixed layout and expectedly accompanies the better performance of location estimation. Similar to section 3.2.1, this section also define some properties inferred from MOM metric in order to promote the GALE algorithm.

Associate (3.27) with (3.26) it can be utilized for representing the MOM metrics in most of the research studies. As Fig. 3.1, the same representation  $\mathbf{x}_k - \mathbf{x}_{i,k} = [\zeta_{i,k} \cos \theta_{i,k}, \zeta_{i,k} \sin \theta_{i,k}]$  for  $i = 1$  to  $N_k$  are used for the coming derivation. Substitut-



ing this equation into (3.10), the MOM value can also be represented as

$$\text{MG}_{\mathbf{x}_k} = \left[ \frac{\sum_{i=1}^{N_k} (\prod_{j=1, j \neq i}^{N_k} r_{j,k}^2)}{\sum_{i=1}^{N_k-1} \sum_{j=i+1}^{N_k} (\prod_{m=1, m \neq i, j}^{N_k} r_{m,k}^2) \sin^2(\theta_{j,k} - \theta_{i,k})} \right]^{\frac{1}{2}} \quad (3.28)$$

And then (3.12) is utilized again to simplify equation (3.28). Consequently, the MOM value in (3.28) can be reformulated as a function of  $\alpha_{i,k}$  as fig. 3.1

$$\text{MG}_{\mathbf{x}_k} = \left[ \frac{\sum_{i=1}^{N_k} (\prod_{j=1, j \neq i}^{N_k} r_{j,k}^2)}{\sum_{i=1}^{N_k-1} \sum_{j=i+1}^{N_k} (\prod_{m=1, m \neq i, j}^{N_k} r_{m,k}^2) \sin^2(\alpha_{ij,k})} \right]^{\frac{1}{2}} \quad (3.29)$$

We can observe an important corollary from the above two equations. MOM value related to both its reference angle and relative distance, however, GDOP is just related to angle. It means that if one of the signal from BS is converted into NLOS, GDOP metric keeps the same value as before. This contradicts the phenomenon, while MOM metric can reflect this effect. Analogous to lemma 2 and lemma 1, minimal MOM values are obtained by considering two different cases (with one degree-of-freedom and with  $N_k$  degree-of-freedom).

**Lemma 3.** For finding minimal attainable MOM, we define the MS located at  $\mathbf{x}_k$  is surrounded by  $N_k$  BSs at  $\mathbf{x}_{i,k}$  (for  $i = 1$  to  $N_k$ ) as shown in Fig. 3.1. And if we let movable BS is  $\ell$ th BS, i.e. the adjustable angle is  $\alpha_{\ell,k}$ ; while the positions for the other BSs are considered fixed. The minimal MOM occurs as the angle  $\alpha_{\ell,k}$  is adjusted to be

$$\alpha_{\ell,k}^m = \frac{1}{2} \tan^{-1} \left( \frac{-\prod_{k=1, k \neq \ell, \ell+1}^{N_k} \zeta_k^2 \sin(2 \sum_{i=1, i \neq \ell-1, \ell}^{N_k} \alpha_{li,k})}{\prod_{k=1, k \neq \ell, \ell+1}^{N_k} \zeta_k^2 \cos(2 \sum_{i=1, i \neq \ell-1, \ell}^{N_k} \alpha_{li,k}) + R} \right) \quad (3.30)$$

$R$  is equal to  $\prod_{k=1, k \neq \ell, \ell+1}^{N_k} \zeta_k^2$  and  $\zeta_0 = \zeta_{N_k}$ . Therefore, the minimal attainable MOM value

w.r.t.  $\mathbf{x}_k$  becomes

$$\text{MG}_{\mathbf{x}_k}^m = \left[ \frac{N_k}{2 \sin^2(\alpha_{\ell,k}^m) + \sum_{i=1, i \neq \ell-1, \ell}^{N_k} \sin^2(\alpha_{i,k})} \right]^{\frac{1}{2}} \quad (3.31)$$

*Proof.* MOM value  $G_{\mathbf{x}_k}$  w.r.t.  $\mathbf{x}_k$  is a function of the angles  $\alpha_{i,k}$  for all  $i = 1$  to  $N_k$ . Analogous to lemma 1 a minimum MOM value will occur under the condition that if only the  $\ell$ th BS (for  $1 \leq \ell \leq N_k$ ) is considered adjustable. It also means the angle  $\alpha_{\ell,k}$  is tunable and  $\alpha_{\ell-1,k} = 2\pi - \alpha_{\ell,k} - \sum_{i=1, i \neq \ell-1, \ell}^{N_k} \alpha_{i,k}$ . Other relative angle are defined to be fixed. The angle  $\alpha_{\ell,k}^m$  which results in the minimal MOM value can therefore be acquired as

$$\alpha_{\ell,k}^m = \arg \left\{ \min_{\forall \alpha_{\ell,k}} \text{MG}_{\mathbf{x}_k}(\alpha_{\ell,k}) \right\} \quad (3.32)$$

It can be observed that (3.32) can be achieved if the following conditions on the first and second derivatives of  $G_{\mathbf{x}_k}$  are satisfied, i.e.

$$\left[ \frac{\partial \text{MG}_{\mathbf{x}_k}(\alpha_{\ell,k})}{\partial \alpha_{\ell,k}} \right]_{\alpha_{\ell,k} = \alpha_{\ell,k}^m} = 0 \quad (3.33)$$

$$\left[ \frac{\partial^2 \text{MG}_{\mathbf{x}_k}(\alpha_{\ell,k})}{\partial^2 \alpha_{\ell,k}} \right]_{\alpha_{\ell,k} = \alpha_{\ell,k}^m} > 0 \quad (3.34)$$

By solving (3.33) and (3.34), the angle  $\alpha_{\ell,k}^m$  can be computed as in (3.30). The minimal MOM value w.r.t.  $\mathbf{x}_k$  can consequently be obtained as in (3.31).  $\square$

**Lemma 4.** *Based on the MOM criterion, if the MS located at  $\mathbf{x}_k$  is surrounded by  $N_k$  BSs at  $\mathbf{x}_{i,k}$  (for  $i = 1$  to  $N_k$ ) as shown in Fig. 3.1 and defining all the BSs are adjustable, all the relative angle  $\alpha_{i,k}$  can be derived as Lemma 3.*

If all the BSs forms a regular polygon, the minimal GDOP value w.r.t.  $\mathbf{x}_k$  is obtained as  $\text{MG}_{\mathbf{x}_k}^m = (\frac{2}{\sqrt{N_k}})\zeta_{i,k}^2$ , which occurs as the angles  $\alpha_{i,k}$  are regulated to be equivalent with each other as  $\alpha_{i,k}^m = 2\pi/N_k$  for all  $i = 1$  to  $N_k$ .

*Proof.* The same deriving procedure can be utilized to derive the MOM. It is shown that it is possible to predict an "optimum" anticipated BS-to-MS geometrical configuration which results in minimum measurement error dilution and minimum least squares position error. Under the definition of MOM, we can acquire angles  $\boldsymbol{\alpha}_k^m \triangleq [\alpha_{1,k}^m \dots \alpha_{i,k}^m \dots \alpha_{N_k,k}^m]$  to meet the minimum MOM value. where

$$\alpha_{i,k}^m = \arg \left\{ \min_{\forall \alpha_{i,k}} \text{MG}_{\mathbf{x}_k}(\boldsymbol{\alpha}_k) \right\} \quad (3.35)$$

If all the relative distances  $\zeta_{i,k}$  are equal for  $i = 1$  to  $N_k$ , GDOP MOM will holds the same conclusion as GDOP. In other words, The minimal GDOP value w.r.t.  $\mathbf{x}_k$  is obtained as

$$\text{MG}_{\mathbf{x}_k}^m = (\frac{2}{\sqrt{N_k}})\zeta_{i,k}^2 \quad (3.36)$$

□

which occurs as the angles  $\alpha_{i,k}$  are regulated to be equivalent with each other as  $\alpha_{i,k}^m = 2\pi/N_k$

**Corollary 2.** *Considering the MS is confined by an  $N_k$ -side regular polygon by placing the  $N_k$  BSs as the vertices of the polygon, the minimal MOM value w.r.t.  $\mathbf{x}_k$  will occur at the center of the regular polygon.*

*Proof.* If we apply the lemma 2 to MOM, it always holds when all the relative distances  $\zeta_{i,k}$  are equal for  $i = 1$  to  $N_k$ . In (3.29) , if all the  $\zeta_{i,k}$  are equal, the minimum value will

occur at the center of the polygon formed by BSs. As the same conclusion as 1, the MS have minimum value at the center of the polygon if all BS form a regular one.  $\square$

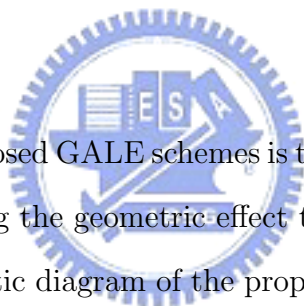
In the next section, the results obtained from both lemmas will be utilized for the design of the proposed GALE algorithms.



# Chapter 4

## Proposed Geometric-Assisted Location Estimation (GALE)

### Algorithms



The main objective of the proposed GALE schemes is to enhance the conventional two-step LS algorithm [5] by considering the geometric effect to the location estimation accuracy. Fig. 4.1 illustrates the schematic diagram of the proposed GALE algorithms. In order to facilitate the location estimation for the MS, three TOA measurements and the location information of the corresponding BSs are considered available to the MS at the time instant  $k$ , i.e.  $\mathbf{r}_k = \{r_{1,k}, r_{2,k}, r_{3,k}\}$  and  $\mathbf{P}_{BS,k} = \{\mathbf{x}_{1,k}, \mathbf{x}_{2,k}, \mathbf{x}_{3,k}\}$ . With the available information, the two-step LS method can acquire the MS's initial location estimate  $\hat{\mathbf{x}}_k^o = [\hat{x}_k^o \ \hat{y}_k^o]$  within two computing iterations.

The GALE algorithms are proposed to further enhance the precision of the initial location estimation of the MS. Based on the available measurement information from the BSs, the concept of the proposed GALE schemes is to acquire the locations of the *fictitious* BSs such as to attain the minimal GDOP value w.r.t the MS's initial location estimate. At the second phase of the GALE schemes, the position information of these

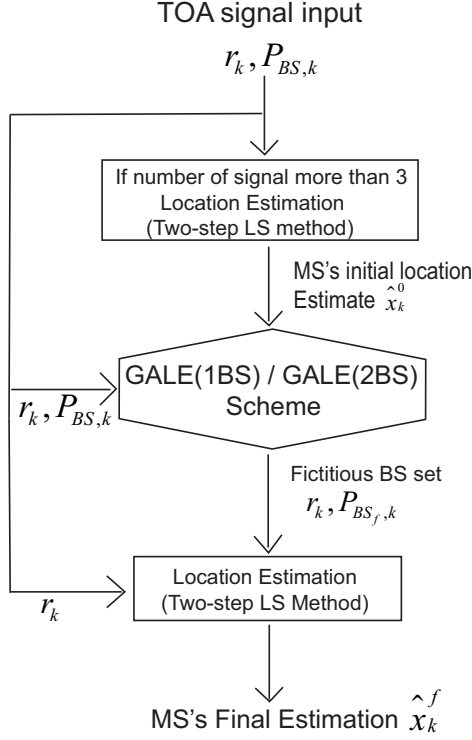


Figure 4.1: Schematic diagram of the proposed GALE algorithms.

*fictitious* BSs will be utilized to replace that of the original BSs in order to achieve better geometric layout for location estimation. Two GALE algorithms, i.e. the GALE(1BS) and GALE(2BS) schemes, are stated as follows.

## 4.1 GALE with One Movable Fictitious BS Scheme

The GALE(1BS) scheme is designed to fictitiously relocate the position of one BS according to the minimal GDOP criterion. Under this condition only one BS is defined to be fictitious movable and others are fixed.

### 4.1.1 GDOP-Assisted (GOLE) Location Estimation Scheme

Without lose of generality, it is considered that  $BS_1$  (i.e.  $\mathbf{x}_{1,k}$ ) is the adjustable BS within the GALE(1BS) scheme. The position of the *fictitious*  $BS_1$  is designed such that the

initial estimated MS ( $\hat{\mathbf{x}}_k^o$ ) will be located at a minimal GDOP position based on the existing geometric layout  $\mathbf{P}_{BS,k} = \{\mathbf{x}_{1,k}, \mathbf{x}_{2,k}, \mathbf{x}_{3,k}\}$ . In other words, based on the initial location estimate  $\hat{\mathbf{x}}_k^o$  associated with the information coming from the BSs (i.e.  $\mathbf{r}_k$  and  $\mathbf{P}_{BS,k}$ ), the three relative angles  $\alpha_{1,k}$ ,  $\alpha_{2,k}$ , and  $\alpha_{3,k}$  between the BSs w.r.t. the MS can be obtained. By adopting the results from Lemma 1, the minimal attainable GDOP  $G_{\hat{\mathbf{x}}_k^o}$  w.r.t. the MS's initial estimate  $\hat{\mathbf{x}}_k^o$  occurs as the angle  $\alpha_{1,k}$  is adjusted as

$$\alpha_{1,k}^m = \frac{1}{2} \tan^{-1} \left( \frac{-\sin(2\alpha_{2,k})}{\cos(2\alpha_{2,k}) + 1} \right) \quad (4.1)$$

It is noted that the angle  $\alpha_{2,k}$  between BS<sub>2</sub> and BS<sub>3</sub> is considered a fixed value; while  $\alpha_{3,k}$  is dependent to the variable angle  $\alpha_{1,k}$ , i.e.  $\alpha_{3,k} = (2\pi - \alpha_{2,k}) - \alpha_{1,k}$ . The following lemma generalizes the solution for the angle  $\alpha_{1,k}^m$  that achieves minimal GDOP value.

**Lemma 5.** *Considering the case that the MS is surrounded by three available BSs, i.e. BS<sub>1</sub>, BS<sub>2</sub>, and BS<sub>3</sub>. It is assumed that only the location of BS<sub>1</sub> is adjustable; while the positions of the other two BSs are considered fixed. The minimal GDOP occurs as BS<sub>1</sub> is situated at the angle that equally bisects the angle formed by BS<sub>2</sub> and BS<sub>3</sub>.*

*Proof.* According to (4.1),  $\alpha_{1,k}^m$  represents the angle that achieves the minimal GDOP value w.r.t. the MS's initial estimate. It is clear to conclude that (4.1) holds if  $\alpha_{2,k} = 2\pi - 2\alpha_{1,k}^m$ . Consequently, the minimal GDOP occurs as BS<sub>1</sub> is positioned at the angle that equally bisects the angle formed by the other two BSs, i.e.

$$\alpha_{1,k}^m = \frac{2\pi - \alpha_{2,k}}{2} \quad (4.2)$$

□

It is observed from Lemma 5 that the fictitiously movable BS<sub>1</sub> should be adjusted such that the angles  $\alpha_{1,k}$  and  $\alpha_{3,k}$  are equal. As a result, the new set of BSs for location

estimation is obtained as  $\mathbf{P}_{BS_f,k}^{(1)} = \{\mathbf{x}_{f1,k}, \mathbf{x}_{2,k}, \mathbf{x}_{3,k}\}$ , where  $\mathbf{x}_{f1,k}$  denotes the location of the *fictitious* BS as

$$\begin{aligned} x_{f1,k} &= r_{1,k} \cos(\theta_{2,k} - \alpha_{1,k}^m) \\ y_{f1,k} &= r_{1,k} \sin(\theta_{2,k} - \alpha_{1,k}^m) \end{aligned} \quad (4.3)$$

where  $\alpha_{1,k}^m$  is obtained from (4.2). The set of updated locations for the BSs  $\mathbf{P}_{BS_f,k}^{(1)}$  associated with the original TOA measurements  $\mathbf{r}_k = \{r_{1,k}, r_{2,k}, r_{3,k}\}$  are exploited to conduct the second-phase two-step LS method as shown in Fig. 4.1. Consequently, the MS's final location estimation  $\hat{\mathbf{x}}_k^f = [\hat{x}_k^f \hat{y}_k^f]$  by adopting the proposed GALE(1BS) scheme can be obtained.

#### 4.1.2 MOM-Assisted (MOLE) Location Estimation Scheme

By using the property of MOM we can design some scheme to implement the system as well. For the mathematical model derived from the chapter 3 . The fictitious position of the adjustable BS can be obtained in order to fit the lowest MOM. Assume that  $BS_1$  is adjustable, the fictitious  $BS_1$  will be relocated at  $x_{1,k}$  in order to make the MS ( $\hat{\mathbf{x}}_k^o$ ) locate at the lowest MOM.

In other words, whenever we get the MS's initial coordinate  $\hat{\mathbf{x}}_k^o$  and the angel  $\alpha_{2,k}$  is considered a fixed value, we can get new fictitious BS set  $P_{BS,k_f}$ . By adopting the results from Lemma 3, the minimal attainable MOM  $G_{\hat{\mathbf{x}}_k^o}$  w.r.t. the MS's initial estimate  $\hat{\mathbf{x}}_k^o$  occurs as the angle  $\alpha_{1,k}$  is adjusted as

$$\alpha_{1,k}^m = \frac{1}{2} \tan^{-1} \left( \frac{-\sin(2\alpha_{2,k})}{\cos(2\alpha_{2,k}) + N} \right) \quad (4.4)$$

the notation  $N$  is equal to  $\left(\frac{r_{3,k}}{r_{2,k}}\right)^2$ , and  $\alpha_{3,k}$  is dependent to the variable angle  $\alpha_{1,k}$ , i.e.



$\alpha_{3,k} = (2\pi - \alpha_{2,k}) - \alpha_{1,k}$ . The following lemma generalizes the solution for the angle  $\alpha_{1,k}^m$  that achieves minimal MOM value.  $\mathbf{P}_{BS_f,k}^{(1)} = \{\mathbf{x}_{f1,k}, \mathbf{x}_{2,k}, \mathbf{x}_{3,k}\}$ , where  $\mathbf{x}_{f1,k}$  denotes the location of the *fictitious* BS as

$$\begin{aligned} x_{f1,k} &= r_{1,k} \cos(\theta_{2,k} - \alpha_{1,k}^m) \\ y_{f1,k} &= r_{1,k} \sin(\theta_{2,k} - \alpha_{1,k}^m) \end{aligned} \quad (4.5)$$

where  $\alpha_{1,k}^m$  is obtained from (4.4). The set of updated locations for the BSs  $\mathbf{P}_{BS_f,k}^{(1)}$  associated with the original TOA measurements  $\mathbf{r}_k = \{r_{1,k}, r_{2,k}, r_{3,k}\}$  are exploited to conduct the second-phase two-step LS method as shown in Fig. 4.1. Consequently, the MS's final location estimation  $\hat{\mathbf{x}}_k^f = [\hat{x}_k^f \hat{y}_k^f]$  by adopting the proposed GALE(1BS) scheme can be obtained.

**Lemma 6.** *We can implement the result derived from MOM to the GALE as well. Assumed that only the location of  $BS_1$  is adjustable. If  $r_{2,k} = r_{3,k}$ , the minimal MOM occurs as  $BS_1$  is situated at the angle that equally bisects the angle formed by  $BS_2$  and  $BS_3$ . Therefore,  $BS_1, BS_2$  and  $BS_3$  forms a isosceles triangle. From this Lemma, it indicates that minimum MOM value occurs when all BSs composing a symmetric layout.*

*Proof.* According to (4.4),  $\alpha_{1,k}^m$  represents the angle that achieves the minimal MOM value w.r.t. the MS's initial estimation. If  $r_{2,k} = r_{3,k}$ ,  $\alpha_{1,k}^m$  will have the same value as (4.1). It also holds the solution  $\alpha_{2,k} = 2\pi - 2\alpha_{1,k}^m$ .

It indicates that  $BS_1$  will forms a isosceles triangle with  $BS_2$  and  $BS_3$  if the distance from MS to  $BS_2$  is equal to distance from MS to  $BS_3$  at this time.  $\square$

### 4.1.3 Coverage-Maximize (CMLE) Location Estimation Scheme

The objective of the proposed GALE algorithms is to utilize the initial location information acquired from the BS to serve as the assisted measurement inputs. Besides, We design

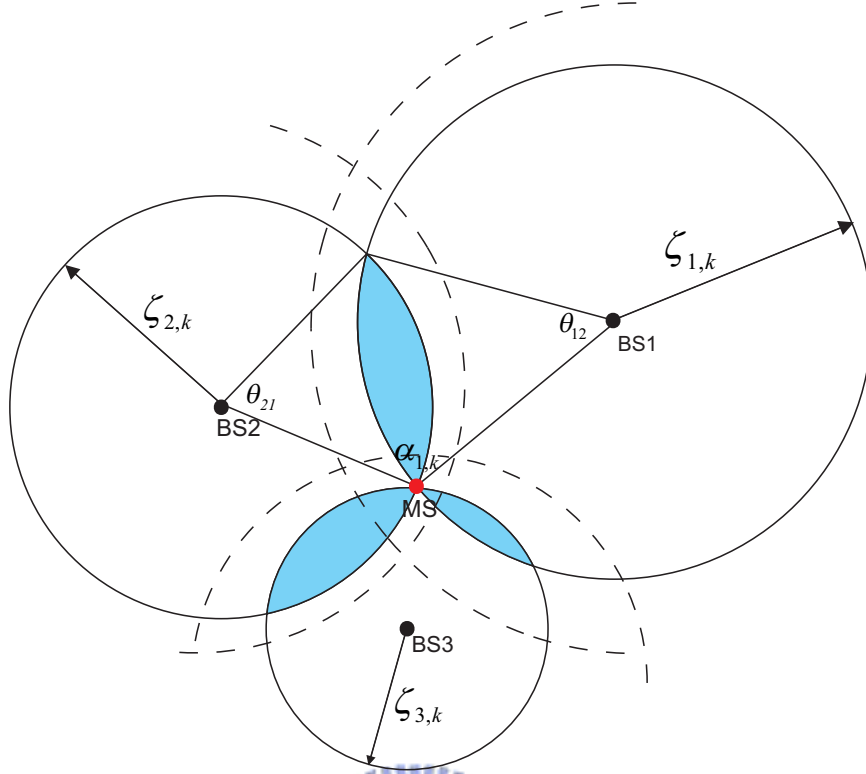


Figure 4.2: The location information for TOA signal

another algorithm to implement the location algorithm. For TOA system as fig.4.2, the error depend on the undetermine region (the area surrounded by dotted line). Because GDOP and MOM are designed in a noise-free environment, we can decrease the region to colored section. The object is to minimize the region and make the total coverage area maximize at the same time. This paper we call it the Coverage Maximum Location Estimation(CMLE).

Analogous to the GALE algorithm by adding geometric constraints within the conventional two-step LS method, the CMLE algorithm extends the concept of "virtual" assistances in the GALE algorithm to add the geometric constraints from the assisted information. The same scheme as GALE, Area model also have 1BS and 2BS scheme. We set  $\mathbf{P}_{BS_f,k}$  in order to make the area of colored region have a minimum value. The value is with respect to both related distance and angle. For example, the cross-section

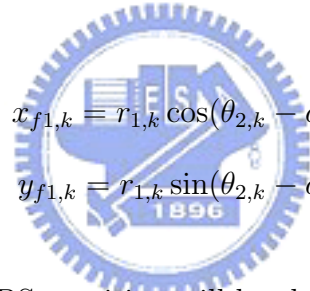
dorm by BS<sub>1</sub> and BS<sub>2</sub> can be expressed as

$$Area = \frac{1}{2} \zeta_{1,k}^2 (\theta_{a1} - \sin \theta_{a1}) \quad (4.6)$$

and  $\theta_{i,1}$  is w.r.t  $\alpha_{i,k}$ . Therefore the total area will be related to  $\alpha_{i,k}$ .

**Corollary 3.** *Following by the GALE 1BS algorithm, each scheme can design its own relocated BS set  $\mathbf{P}_{BS_f,k}^{(2)} = \{\mathbf{x}_{f1,k}, \mathbf{x}_{f2,k}, \mathbf{x}_{f3,k}\}$  as above scheme shows. For the circumstance that  $\zeta_{2,k} = \zeta_{3,k}$ , the proposed BS set  $\mathbf{P}_{BS_f,k}^{(2)}$  will have the same position.*

*Proof.* Assume all the relative distance are equal, we can take this data into each scheme. When  $\zeta_{2,k} = \zeta_{3,k}$ , the proposed answer  $\alpha_{i,k}^m$  will have same solution of  $\alpha_{1,k} = \frac{2\pi - \alpha_{2,k}^m}{2}$ . As we have defined before,



$$\begin{aligned} x_{f1,k} &= r_{1,k} \cos(\theta_{2,k} - \alpha_{1,k}^m) \\ y_{f1,k} &= r_{1,k} \sin(\theta_{2,k} - \alpha_{1,k}^m) \end{aligned} \quad (4.7)$$

This equation shows that the BS<sub>1</sub> position will be the same. □

## 4.2 GALE with Two Movable Fictitious BSs Scheme

According to Lemma 2 and 4, more degree of freedom can be set. For the purpose of location, 3 BSs is sufficient to locate a 2-D MS. For this reason we just set 3 BSs and let all BS be adjustable (i.e. two BSs can be relative adjusting). The below schemes are the designed method by combing geometric property.

### 4.2.1 GDOP-Assisted (GOLE) Location Estimation Scheme

In order to achieve the minimal GDOP for the existing geometric layout, the GALE(2BS) scheme is designed by considering the case while all the BSs are fictitiously movable. By adopting the results from Lemma 2, it can be obtained that the angles  $\alpha_{i,k}$  that achieve the minimal GDOP value are determined to be  $\alpha_{i,k}^m = 2\pi/N_k = 2\pi/3$  for  $i = 1$  to 3. In other words, the three BSs are fictitiously adjusted such that equally partitioned angles are observed.

Therefore, the set of *fictitious* BSs by exploiting the GALE(2BS) scheme is represented as  $\mathbf{P}_{BS_f,k}^{(2)} = \{\mathbf{x}_{f1,k}, \mathbf{x}_{f2,k}, \mathbf{x}_{f3,k}\}$ , where  $\mathbf{x}_{fi,k}$  (for  $i = 1$  to 3) indicates the locations of the *fictitious* BSs. It is noted that  $\mathbf{x}_{f1,k}$  is selected to be  $\mathbf{x}_{1,k}$  as the rotation reference. Consequently, the locations of the other two *fictitious* BSs can be acquired as

$$\begin{aligned} x_{fi,k} &= r_{i,k} \cos(\theta_{1,k} + \sum_{s=1}^{i-1} \alpha_{s,k}^m) \\ y_{fi,k} &= r_{i,k} \sin(\theta_{1,k} + \sum_{s=1}^{i-1} \alpha_{s,k}^m) \end{aligned} \quad (4.8)$$

for  $i = 2$  and 3. Similar to the GOLE(1BS) scheme, the *fictitious* locations of the BSs  $\mathbf{P}_{BS_f,k}^{(2)}$  associated with the TOA measurements  $\mathbf{r}_k$  are utilized to serve as the new set of measurement inputs for the two-step LS method at the second stage. As a result, the final location estimate of the MS (i.e.  $\hat{\mathbf{x}}_k^f$ ) can be acquired.

### 4.2.2 MOM-Assisted (MOLE) Location Estimation Scheme

For GDOP MOM metric, by adapting lemma1 we get the result for  $\alpha_{i,k}^m$ . Because GDOP MOM metric is depends on both distance and related angle, its solution is more complex.

We first define the determine function  $D_f$ ,

$$D_f = B^2 - 4AC \quad (4.9)$$

$$A = \frac{a^2}{b^2c^2} - \frac{a^2}{b^2}, B = \frac{2a^2}{bc^2}, C = \frac{a^2}{c^2} + \frac{a^2}{b^2} - 1 \text{ and } a = r_{3,k}^2, b = r_{1,k}^2 \text{ and } c = r_{2,k}^2$$

if  $D_f \geq 0$ , the solution will be derived as

$$\alpha_{1,k}^m = 0.5 \times \arccos\left(\frac{-B + \sqrt{D_f}}{2A}\right) \quad (4.10)$$

and

$$\alpha_{2,k}^m = 0.5 \times \arcsin\left(\frac{a}{b} \sin(2\alpha_{1,k}^m)\right) \quad (4.11)$$

if  $D_f \leq 0$ , the minimum value will occur under the condition: the angle  $\alpha_{i,k}^m$  corresponded to the largest  $\zeta_{i+2,k}$  will be  $\pi/2$ ; and the angle corresponded to smallest  $\zeta_{i+2,k}$  will be  $\pi$ .

Similar to the GALE (1BS) scheme, the *fictitious* locations of the BSs  $\mathbf{P}_{BS_f,k}^{(2)}$  associated with the TOA measurements  $\mathbf{r}_k$  are utilized to serve as the new set of measurement inputs for the two-step LS method at the second stage. As a result, the final location estimate of the MS (i.e.  $\hat{\mathbf{x}}_k^f$ ) can be acquired. It is noted that the noiseless relative distances  $\zeta_{i,k}$  in (3.9) are approximately replaced by  $r_{i,k}$  since  $\zeta_{i,k}$  are considered unattainable.

### 4.2.3 Coverage-Maximize (CMLE) Location Estimation Scheme

When all the BSs are assigned to be movable, the CMLE 2BS scheme is continuous computing the relative angle  $\alpha_{i,k}$  in order to make the total overlapping area  $A_{x_k}$  to be minimum. It can be expressed as

$$\alpha_{i,k}^m = \arg \left\{ \min_{\forall \alpha_{i,k}} A_{x_k}(\boldsymbol{\alpha}_k) \right\} \quad (4.12)$$

for  $i=1$  to 3.

**Corollary 4.** *Following by the GALE 2BS algorithm, each scheme can design its own relocated BS set  $\mathbf{P}_{BS_f,k}^{(2)} = \{\mathbf{x}_{f1,k}, \mathbf{x}_{f2,k}, \mathbf{x}_{f3,k}\}$  as above scheme shows. For the circumstance that all the relative distance are equal, the proposed BS set  $\mathbf{P}_{BS_f,k}^{(2)}$  will have the same position.*

*Proof.* Assume all the relative distance are equal, we can take this data into each 2BS scheme. All the proposed answer  $\alpha_{i,k}^m$  will have same solution of  $\pi/3$ . As we have defined before,

$$\begin{aligned} x_{fi,k} &= r_{i,k} \cos(\theta_{1,k} + \sum_{s=1}^{i-1} \alpha_{s,k}^m) \\ y_{fi,k} &= r_{i,k} \sin(\theta_{1,k} + \sum_{s=1}^{i-1} \alpha_{s,k}^m) \end{aligned} \quad (4.13)$$

for  $i = 2$  and 3. This equation shows that all the BSs's position will be the same.  $\square$

# Chapter 5

## Performance Evaluation

Simulations are performed to show the effectiveness of the GALE algorithms under different network topologies and the MS's positions. The proposed GALE(1BS) and GALE(2BS) schemes are compared with the exiting two-step LS and the TSE algorithms. As shown in Fig. 5.1, two different types of geometric layouts are designed to validate the effectiveness of the proposed GALE algorithms. The left plot illustrates the case while the MS is located at a better geometric layout,

### 5.1 Noise Models

Different noise models [22] are considered in the simulations in order to represent the environments with both the LOS and the NLOS signals. The model for the measurement noise of the TOA signals is selected as the Gaussian distribution with zero mean and 10 meters of standard deviation, i.e.  $n_{i,k} \sim \mathcal{N}(0, 100)$ . On the other hand, an exponential distribution  $p_{e_{i,k}}(\tau)$  is assumed for the NLOS noise model of the TOA measurements as

$$p_{e_{i,k}}(v) = \begin{cases} \frac{1}{\lambda_{i,k}} \exp\left(-\frac{v}{\lambda_{i,k}}\right) & v > 0 \\ 0 & \text{otherwise} \end{cases} \quad (5.1)$$

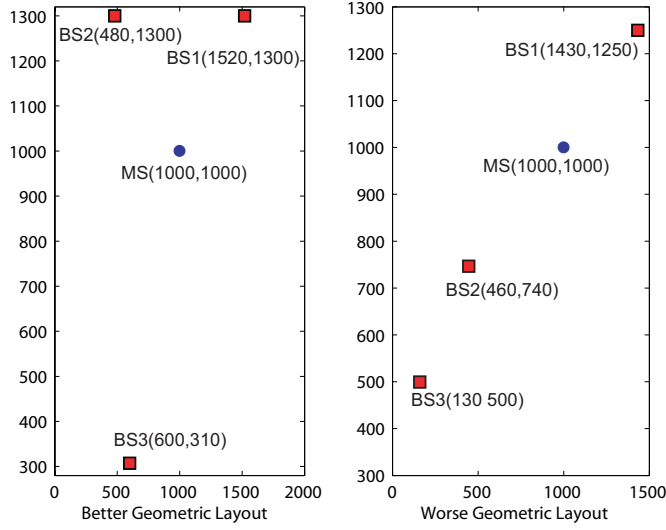


Figure 5.1: Network topologies for performance evaluation (left plot: better geometric layout with  $G_{x_k}^g = 1.2253$  and  $MG_{x_k}^g = 796.79$ ; right plot: worse geometric layout with  $G_{x_k}^b = 13.884$  and  $MG_{x_k}^b = 8389.2$ ).

where  $\lambda_{i,k} = c \cdot \tau_{i,k} = c \cdot \tau_m (\zeta_{i,k})^\varepsilon \rho$ . The parameter  $\tau_{i,k}$  is the RMS delay spread between the  $i$ th BS to the MS, and  $\tau_m$  represents the median value of  $\tau_{i,k}$ .  $\varepsilon$  is the path loss exponent which is assumed to be 0.5, and the factor for shadow fading  $\rho$  is set to 1 in the simulations. It is noted that the parameters for the noise models as listed in this subsection primarily fulfill the environment while the MS is located within the rural area.

## 5.2 Simulation Results

Fig. 5.2 illustrates the performance comparison between these schemes under the LOS environment with both better and worse geometric layouts, i.e. left with  $G_{x_k}^b = 1.22$  and right with  $G_{x_k}^w = 13.88$ . It is noted that the Estimation error of the MS's position is represented as  $\Delta \hat{\mathbf{x}} = \|\hat{\mathbf{x}}_k^f - \mathbf{x}_k\|$ , where  $\hat{\mathbf{x}}_k^f$  indicates the MS's final estimate from the location estimation algorithms. It can be observed that the proposed GALE algorithms outperform the other two existing schemes, especially under the worse geometric environ-



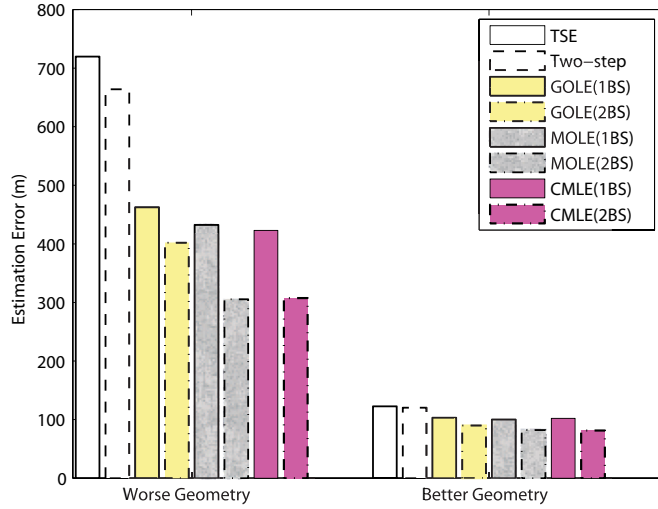


Figure 5.2: Performance comparison under the LOS environment with both better (left:  $G_{x_k}^b = 1.22$ ) and worse (right:  $G_{x_k}^w = 13.88$ ) geometric layouts.

ment. Considering the layout with larger GDOP value (i.e.  $G_{x_k}^w = 13.88$ ) as shown in Fig. 5.3, the comparison for the Estimation errors versus the standard deviations of the measurement noises is illustrated. It can be seen that the proposed GALE(2BS) scheme can provide the smallest Estimation errors comparing with the other algorithms.

Figs. 5.4 and 5.5 illustrates the case for performance comparison under the NLOS environment. It is noted that Fig. 5.5 is illustrated by observing the Estimation errors versus the median values of the NLOS noises (i.e.  $\tau_m$ ). It can still be observed that the proposed GALE(2BS) scheme outperforms the other algorithms even under the existence of the NLOS errors, i.e. around 250 m less in Estimation error compared to the two-step LS method with  $\tau_m = 0.3$ . Moreover, the benefits by fictitiously adjusting the locations of two BSs compared to that for one BS can also be observed in both the LOS and the NLOS environments. With the incorporation of the geometric information into the location estimation, the merits of the proposed GALE schemes can be observed.

Table1 shows the performance comparison between the Location Estimation Schemes

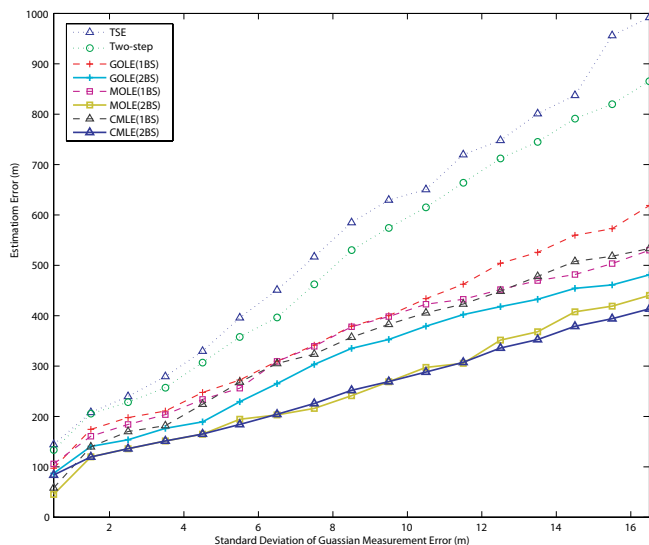


Figure 5.3: Performance comparison under the LOS environment with worse geometric layout ( $C_T^{x_k^w} = 13.88$ ): Estimation error v.s. standard deviation of measurement noise.

under LOS environment. while the MS is located far from its BSs. It can be seen from plots that the proposed GALE(1BS) scheme outperforms the conventional two-step LS method with more than 100 m of estimation error under 90% of average position errors. GALE(2BS) scheme can outperform even more to 250 m than two-step LS method (noise standard deviation= 10). Table2 shows the performance comparisons between the Location Estimation Schemes under NLOS environment (median value  $\tau_m = 0.3$ ). The proposed GALE(1BS) algorithm improve more than the environment under LOS. For example, under 90% of average position error the GALE(1BS) scheme can mitigate 170 m more than two-step LS and GALE(2BS) scheme can mitigate about 300 m.

From figs. 5.4, we can also improve that MOLE and CMLE outperform that GALE especially under NLOS environment. GDOP metric is derived in chapter3 and is independent of relative distance. Under NLOS environment the distance error is increasing rapidly with the relative distance, therefore the other two GALE can observe this factor. However, CMLE waste more computation than MOLE, we can get the conclusion that

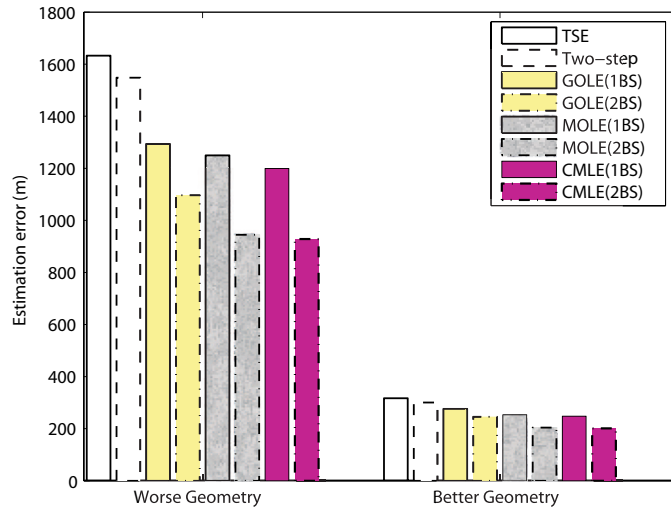


Figure 5.4: Performance comparison under the NLOS environment with both better (left:  $G_{x_k}^b = 1.22$ ) and worse (right:  $G_{x_k}^w = 11.08$ ) geometric layouts ( $\tau_m = 0.3$ ).

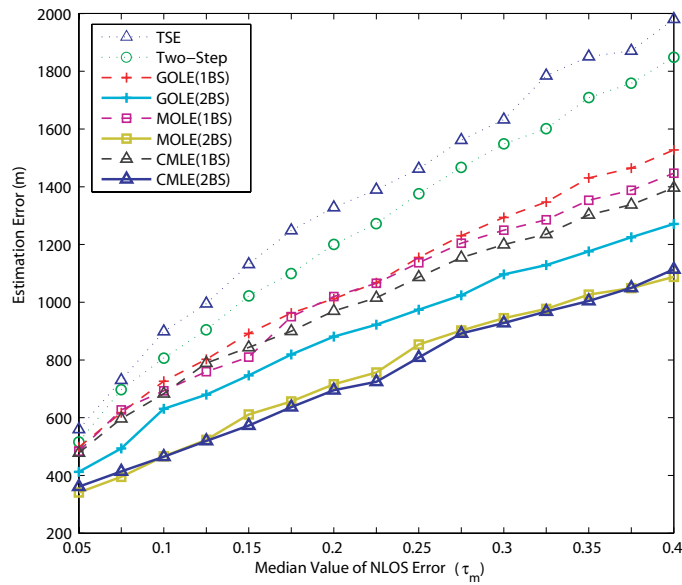


Figure 5.5: Performance comparison under the NLOS environment with worse geometric layout ( $G_{x_k}^w = 13.88$ ): Estimation error v.s. median value of NLOS noise.

TABLE I

Performance Comparisons between the Location Estimation Schemes in LOS: Estimation Error (m)

	10%	20%	30%	40%	50%	60%	70%	80%	90%	100%
TSE	103.12	138.61	201.12	258.56	371.87	394.25	458.19	525.51	562.69	711.56
Two-step LS	93.951	148.69	198.72	248.81	301.87	358.15	418.99	485.63	562.69	691.76
GOLE(1BS)	67.439	102.08	133.78	165.44	198.84	235.27	273.81	316.73	367.8	446.87
GOLE(2BS)	55.452	82.652	108.95	135.43	162.23	192.07	225.64	263.02	307.58	390.05
MOLE(1BS)	61.365	92.18	121.69	151.74	182.55	216.78	254.71	297.6	346.9	434
MOLE(2BS)	49.388	71.762	92.532	112.77	133.39	155.91	181.36	210.17	244.18	297.56
CMLE(1BS)	61.072	89.807	119.44	148.89	188.95	221.84	259.29	301.44	351.03	429.16
CMLE(2BS)	44.878	65.227	84.109	102.49	121.23	141.7	164.83	191	221.91	270.38

TABLE 2

Performance Comparisons between the Location Estimation Schemes in NLOS: Estimation Error (m)

	10%	20%	30%	40%	50%	60%	70%	80%	90%	100%
TSE	229.29	418.74	505.94	669.6	709.4	834.8	957.7	1082.4	1214.4	1633.6
Two-step LS	207.81	332.68	405.49	556.55	685.58	701.4	814.8	929.9	1051.7	1554.1
GOLE(1BS)	145.34	265.82	371.63	463.64	547.54	622.76	691.04	760.95	836.24	1296.29
GOLE(2BS)	110.35	242.58	350.7	384.88	407.33	420.24	586.77	651.89	719.73	1123.3
MOLE(1BS)	132.33	256.7	358.49	443.49	546.03	627.03	682.67	726.37	794.32	1226.9
MOLE(2BS)	115.34	230.27	331.52	378.59	390.89	403.46	527.83	592.9	661.49	960.93
CMLE(1BS)	138.57	265.9	362.46	428.97	507.83	575.12	649.01	723.77	790.3	1200.3
CMLE(2BS)	114.88	229.05	330.48	387.33	393.65	462.4	526.81	591.62	659.36	946.39

MOLE is the best choice under NLOS environment.

# Chapter 6

## Conclusion

The NLOS errors will cause large positive biases while measuring the time information data. The inaccuracies of the range measurements consequentially make the conventional location algorithms, like the two-step LS method [5], fail to estimate the MS's position. The location estimation algorithms with the assistance from the geometric property are presented in this paper. Since it can be indicated from chapter 2 and chapter 3 that the location error has big concern with the geometry, the proposed GALE methods which intend to make the MS be at the location where the geometry distribution is the optimum. Six geometric-assisted location estimation (GALE) algorithms are proposed by considering the geometric layouts between the mobile station and its associated base stations. The geometry information such as GDOP, MOM and coverage have been utilized to fictitiously relocate the positions of the BSs in order to obtain a better geometric layout for location estimation. It is shown in the simulation results that the proposed GALE schemes can provide consistent accuracy for location estimation, especially under the environments with poor geometric layout.

# Bibliography

- [1] Y. Zhao, "Standardization of Mobile Phone Positioning for 3G Systems," *IEEE Commun. Mag.*, vol. 40, no. 7, pp.108–116, Jul 2002.
- [2] L. Perusco and K. Michael, "Control, Trust, Privacy, and Security: Evaluating Location-based Services," *IEEE Technol. Soc. Mag.*, vol. 26, no. 1, pp. 4–16, 2007.
- [3] N. Patwari, J. Ash, S. Kyperountas, I. Hero, A.O., R. Moses, and N. Correal, "Locating the Nodes: Cooperative Localization in Wireless Sensor Networks," *IEEE Signal Processing Mag.*, vol. 22, no. 4, pp. 54–69, July 2005.
- [4] W. Foy, "Position-Location Solutions by Taylor-Series Estimation," *IEEE Trans. Aerosp. Electron. Syst.*, vol. 12, pp. 187–194, March 1976.
- [5] K. Chan, Y.T. Ho, "A Simple and Efficient Estimator for Hyperbolic Location," *IEEE Trans. Acoust., Speech, Signal Processing*, vol. 42, pp. 1905–1915, Aug 1994.
- [6] G. Changlin Ma Klukas, R. Lachapelle, "An Enhanced Two-Step Least Squared Approach for TDOA/AOA Wireless Location," *IEEE International Conf. on Communications (ICC '03)*, vol. 2, pp. 987–991, May 2003.
- [7] J. Caffery, J.J., "A New Approach to the Geometry of TOA Location," *IEEE Vehicular Technology Conf.(VTC-Fall)*,vol. 4, pp. 1943–1949, Sep 2000.

- [8] N. Levanon, "Lowest GDOP in 2-D Scenarios," in *Proc. IEE Radar, Sonar and Navigation*, vol. 147, pp. 149 - 153, June 2000.
- [9] Kadar, I. "Optimum Geometry Selection for Sensor Fusion." In Proceedings of SPIE, 3374 (Apr. 1998), 96X107. 4393 (Apr. 2001).
- [10] J. Chaffee, and J. Abel, "GDOP and the Cramer-Rao Bound," in *Proc. IEEE Position Location and Navigation Symposium*, pp. 663 - 668, Apr. 1994.
- [11] R. J. Kelly, "Reducing Geometric Dilution of Precision Using Ridge Regression," *IEEE Trans. Aerospace and Electronic Systems*, pp. 154 - 168, Vol. 26, Jan. 1990.
- [12] J. Caffery Jr. and G. L. Stuber, "Subscriber Location in CDMA Cellular networks," *IEEE Trans. Veh. Technol.*, vol.47, pp.406-416, May 1998.
- [13] M. I. Silventoinen, T. Rantalainen, "Mobile Station Emergency Locating in GSM," *IEEE International Conference on Personal Wireless Communications*, India, Feb. 1996.
- [14] S. Venkatraman, J. J. Caffery, and H. R. You, A Novel TOA Location Algorithm using LOS Range Estimation for NLOS Environments, *IEEE Trans. Veh. Technol.*, vol. 53, no. 5, pp. 1515V1524, Sep. 2004.
- [15] Chen, C., Feng, K., Chen, C., Tseng, P., "Wireless Location Estimation with the Assistance of Virtual Base Stations ", *Vehicular Technology, IEEE Transactions* , 2003 Page(s):1 - 1
- [16] R. O. Schmidt, "Multiple Emitter Location and Signal Parameter Estimation," *IEEE Trans. Antennas and Propagation*, Vol. 34, Issue 3, pp. 276-280, Mar. 1986.



- [17] E. G. Strom, S. Parkvall, S. L. Miller, and B. E. Ottersten, "Propagation Delay Estimation of DS-CDMA Signals in a Fading Environment," *IEEE GLOBECOM.*, pp. 85-89, Nov. 1994.
- [18] B. M. Radich and K. M. Buckley, "The Effect of Source Number Underestimation on MUSIC Location Estimates," *IEEE Trans. on Signal Processing*, Vol. 42, pp. 233-236, Jan. 1994.
- [19] Y. T. Chan, C. H. Yau, and P. C. Yau, "Linear and Approximate Maximum Likelihood Localization from TOA Measurements," *IEEE Signal Processing and Its Applications*, Vol. 2, pp. 295-298, Jul. 2003.
- [20] X. Wang, Z. Wang, and B. O'Dea, "A TOA-Based Location Algorithm Reducing the Errors due to Non-Line-of-Sight (NLOS) Propagation," *IEEE Trans.*, Vol. 52, Jan. 2003.
- [21] L. Cong, and W. Zhuang, "Hybrid TDOA/AOA Mobile User Location for Wideband CDMA Cellular Systems," *IEEE Trans. Wireless Communications*, Vol. 1, pp. 439-437, Jul. 2002.
- [22] P. C. Chen, "A Non-Line-of-Sight Error Mitigation Algorithm in Location Estimation," *Proc. IEEE Wireless Communication and Networking Conf.*, pp. 316-320, Sep. 1999.
- [23] M. P. Wylie and J. Holtzman, "The Non-Line of Sight Problem in Mobile Location Estimation," *Proc. IEEE Int. Conf. Universal Personal Communications*, Vol.2, pp.827-831, Sep. 1996.
- [24] J. Borras, P. Hatrack and N. B. Mandayam, "Decision Theoretic Framework for NLOS Identification," *VETEC*, Vol. 2, pp.1583 - 1587, May 1998.





- [25] B. L. Le, K. Ahmed, and H. Tsuji, "Mobile Location Estimation with NLOS Mitigation Using Kalman Filtering," *WCNC*, Vol 3, pp.1969-1973, Mar. 2003.
- [26] S. Venkatraman, J. Caffery, Jr., and H.-R. You, "A Novel ToA Location Algorithm Using LoS Range Estimation for NLoS Environments," *IEEE Trans. on Vehicular Technology*, Vol. 53, Issue 5, pp. 1515-1524, Sep. 2004.
- [27] C. L. Chen and K. T. Feng, "An Efficient Geometry-Constrained Location Estimation Algorithm for NLOS environments," *Wireless Networks, Communications and Mobile Computing, 2005 International Conference*, vol.1, pp.244-249, Jun. 2005.
- [28] L. J. Greenstein, V. Erceg, Y. S. Yeh, and M. V. Clark, "A New Path-Gain/ Delay-Spread Propagation Model for Digital Cellular Channels," *IEEE Trans. on Vehicular Technology*, Vol. 46, pp. 477-485, May 1997.

